CNWRA 94-021

THERMO-HYDRO-MECHANICAL COUPLED MODELING: BIG-BEN EXPERIMENT, TC3

DECOVALEX—PHASE III

Prepared for

Nuclear Regulatory Commission
Contract NRC-02-93-005

Prepared by

Center for Nuclear Waste Regulatory Analyses
San Antonio, Texas

September 1994

THERMO-HYDRO-MECHANICAL COUPLED MODELING: BIG-BEN EXPERIMENT, TC3

DECOVALEX - PHASE III

Prepared for

Nuclear Regulatory Commission
Contract NRC-02-93-005

Prepared by

Mikko P. Ahola
Goodluck I. Ofoegbu
Asadul H. Chowdhury
Sui-Min (Simon) Hsiung

Center for Nuclear Waste Regulatory Analyses
San Antonio, Texas

September 1994

PREVIOUS REPORTS IN SERIES

Number	Name	Date Issued
CNWRA 90-004	Qualification Studies on the Distinct Element Code UDEC Against Some Benchmark Analytical Problems	January 1990
CNWRA 90-006	Qualification Studies on the Finite Element Code HONDO II Against Some Benchmark Analytical Problems	February 1990
CNWRA 92-005	Thermo-Hydro-Mechanical Coupled Modeling: Multiple Fracture Model, BMT2 Coupled Stress — Flow Model, TC1 DECOVALEX — PHASE I	April 1992
CNWRA 93-002	Thermo-Hydro-Mechanical Coupled Modeling: Near Field Repository Model, BMT3 DECOVALEX — PHASE II	August 1993
CNWRA 93-024	Evaluation of Rock Joint Models and Computer Code UDEC Against Experimental Results	December 1993

ABSTRACT

This report presents results of a finite element analysis for one of the test case (TC) problems identified for modeling during Phase III activities of the international cooperative project DECOVALEX (acronym for the **DE**velopment of **CO**upled models and their **VAL**idation against **EX**periments in nuclear waste isolation). The analysis was conducted for the TC problem called the Big-Ben Experiment (TC3) using the commercially available finite element code ABAQUS with the option of two types of discrete joint elements. The Big-Ben Experiment was designed to evaluate the heat transfer, water uptake, and swelling behavior in an engineered barrier system for underground disposal of high-level nuclear waste. The engineered barrier system consists of an electric heater, a carbon steel overpack, clay buffer material, and a cylindrical reinforced concrete block with a hole at the center. The buffer material between the overpack and concrete consisted of a partially saturated bentonite clay and sand mixture. The experiment consists of uniform heating and water injection into a thin gap between the buffer and concrete for a time period of 5 months. The ABAQUS results show good agreement with the experimental measurements of temperatures within the engineered barrier system. Comparison of the volumetric water content within the buffer material also shows fairly good agreement, however, ABAQUS appears to overpredict the water content near the innermost region of the buffer material. The reason for this overprediction is that ABAQUS cannot simulate the drying effect that takes place near the heater as a results of moisture being driven away from the regions of higher temperature. ABAQUS can monitor only the liquid phase (i.e., wetting fluid) and not the gas phase. The biggest disagreement between the numerical and experimental results appears to be in the radial and vertical stress components. ABAQUS appears to incorrectly predict tension in the outer regions of the buffer adjacent to the concrete. The reason for this phenomenon is possibly due to the high suction combined with the low stiffness properties of the bentonite. Future analyses may find it more appropriate to use interface elements rather than continuum elements to model the gap region. These interface elements would allow separation to occur between the bentonite and concrete, and likely eliminate the tension. Also, it may be more appropriate in the future to model the bentonite as an inelastic (i.e., elastic-plastic) material with swelling versus a purely elastic material with swelling. Final comparison and discussion of modeling results obtained by various research teams of DECOVALEX, that will be published in the DECOVALEX Phase III final report by the Swedish Nuclear Power Inspectorate, may provide additional insight regarding this behavior.

(THIS PAGE INTENTIONALLY LEFT BLANK)

CONTENTS

Section Page

FIGURES . . . vi
TABLES . . . vii
ACKNOWLEDGMENTS . . . ix
QUALITY OF DATA . . . ix
SOFTWARE QUALITY ASSURANCE . . . ix
EXECUTIVE SUMMARY . . . xi

1 INTRODUCTION . . . 1-1
1.1 BACKGROUND . . . 1-1
1.2 DECOVALEX PROBLEMS: PHASE III . . . 1-1
1.3 COMPUTER PROGRAMS FOR THM PROCESSES . . . 1-3
1.4 OBJECTIVE AND STRUCTURE OF THE REPORT . . . 1-3

2 BRIEF DESCRIPTION OF THE ABAQUS CODE . . . 2-1

3 MATHEMATICAL BACKGROUND OF THE ABAQUS CODE . . . 3-1
3.1 THERMAL ANALYSIS . . . 3-1
3.2 COUPLED PORE FLUID DIFFUSION AND STRESS ANALYSIS . . . 3-1

4 BIG-BEN EXPERIMENT . . . 4-1
4.1 BRIEF DESCRIPTION OF THE PROBLEM . . . 4-1
4.2 DEFINITION OF INPUT PARAMETERS . . . 4-1
4.3 ABAQUS MODELING APPROACH . . . 4-8
4.4 COMPUTER HARDWARE AND TIME REQUIREMENTS . . . 4-11

5 COMMENTS ON THE GIVEN SPECIFICATIONS FOR THE TC3 PROBLEM . . . 5-1

6 RESULTS . . . 6-1

7 DISCUSSION OF THE RESULTS . . . 7-1

8 RECOMMENDATIONS . . . 8-1

9 SUMMARY AND CONCLUSIONS . . . 9-1

10 REFERENCES . . . 10-1

APPENDIX A — ABAQUS INPUT FILE FOR THE TC3 PROBLEM (THERMAL ANALYSIS)
APPENDIX B — ABAQUS INPUT FILE FOR THE TC3 PROBLEM (POROELASTIC ANALYSIS)
APPENDIX C — TABULAR OUTPUT FROM ABAQUS FOR THE TC PROBLEM

FIGURES

Figure | Page

4-1 Schematic view of Big-Ben experiment equipment 4-2
4-2 Schematic view of Big-Ben experiment equipment (buffer material) 4-3
4-3 Moisture retention curve used by ABAQUS for the bentonite as determined from fitting experimental data to the Van Genuchten relationship 4-6
4-4 Relationship between relative conductivity and saturation used by ABAQUS for the bentonite as determined from Van Genuchten relationships 4-7
4-5 ABAQUS axisymmetric finite element mesh 4-9

6-1 Comparison of temperatures at a depth 3,000 mm below the ground surface (GL-3000) corresponding to the mid-height of the heater 6-2
6-2 Comparison of volumetric water contents through the buffer at a depth 1,500 mm below the ground surface (GL-1500) 6-3
6-3 Comparison of volumetric water contents through the buffer at a depth 2,350 mm below the ground surface (GL-2350) 6-6
6-4 ABAQUS results for the saturation through the buffer at a depth 3,000 mm below the ground surface (GL-3000), after elapsed times of 1 and 5 months 6-7
6-5 ABAQUS results for the void ratio through the buffer at a depth 3,000 mm below the ground surface (GL-3000), after elapsed times of 1 and 5 months 6-8
6-6 ABAQUS results for the radial stress through the buffer at a depth 3,000 mm below the ground surface (GL-3000), after elapsed times of 1 and 5 months 6-9
6-7 ABAQUS results for the vertical stress through the buffer at a depth 3,000 mm below the ground surface (GL-3000), after elapsed times of 1 and 5 months 6-10
6-8 ABAQUS mesh plot of the buffer region showing a) initial undeformed mesh, and b) deformed mesh after a time of 1 month (displacement magnification factor = 20) . . . 6-11

TABLES

Table Page

4-1 Properties of buffer material composed of a 70-percent bentonite and 30-percent quartz sand mixture compacted to a dry density of 1.6 g/cm^3 4-4
4-2 Input parameters used in the analysis 4-8

(THIS PAGE INTENTIONALLY LEFT BLANK)

ACKNOWLEDGMENTS

The authors would like to thank Drs. Randall D. Manteufel and Amitava Ghosh for their technical reviews and Dr. Wesley C. Patrick for his programmatic review of this document. In addition, the authors would like to thank Mr. Jacob Philip of the Nuclear Regulatory Commission (NRC) for providing coordination between the Center for Nuclear Waste Regulatory Analyses (CNWRA) research team and the DECOVALEX Secretariat. The authors are also thankful to Rebecca A. Sanchez and Cathy Garcia for skillful typing of the report, and to Corky Gray, who provided a full range of expert editorial services in the preparation of the final document.

This report was prepared to document work performed by the CNWRA for the NRC under Contract NRC-02-93-005. The activities reported here were performed on behalf of the NRC Office of Nuclear Regulatory Research, Division of Regulatory Applications. This report is an independent product of the CNWRA and does not necessarily reflect the views or regulatory position of the NRC.

QUALITY OF DATA

CNWRA-generated original data contained in this report meet quality assurance requirements described in the CNWRA Quality Assurance Manual. Sources for other data should be consulted for determining the level of quality for those data.

SOFTWARE QUALITY ASSURANCE

The finite element computer code ABAQUS is commercially available. The CNWRA does not have access to its source code; therefore, it is not controlled under the CNWRA Software Configuration Procedures.

(THIS PAGE INTENTIONALLY LEFT BLANK)

EXECUTIVE SUMMARY

Simulation of the thermal-hydrological-mechanical (THM) behavior of the test case (TC) problem identified as the Big-Ben Experiment (TC3) is presented herein as a part of the Phase III activities of the international cooperative project DECOVALEX (acronym for the **DE**velopment of **CO**upled models and their **VAL**idation against **EX**periments in nuclear waste isolation). The analysis was conducted using the commercially available finite element code ABAQUS. The primary objectives of the DECOVALEX study are to validate coupled THM models believed to be important to the licensing of a high-level nuclear waste (HLW) repository, as well as to identify the needs for further development of the computer codes based on the importance of various coupling mechanisms. The DECOVALEX study includes both benchmark test (BMT) and TC problems. The BMT problems are used to compare the results from different computer codes capable of modeling THM behavior. The TC problems are used to compare the computer code results with those from actual experiments that have been designed for the DECOVALEX study. Five TC problems were selected by the DECOVALEX Secretariat for the DECOVALEX Phase III study. The Center for Nuclear Waste Regulatory Analyses (CNWRA) research team has analyzed the TC3 problem during Phase III, which is the focus of this report.

The Big-Ben Experiment was designed to simulate a typical engineered barrier system based on the current design in the Japanese HLW disposal program. The simulated engineered barrier system is composed of an electric heater, a carbon steel overpack, buffer material, and cylindrical concrete block with a borehole. The reinforced concrete containment for the experiment has an outside diameter of 6 m and is 5 m in height. A borehole approximately 1.7 m in diameter and 4.5 m in depth is located in the center of the reinforced concrete containment. An electric heater with three cartridge heaters is set in the overpack, which is about 1 m in diameter and 2 m in height. The buffer material lying between the overpack and reinforced concrete containment consists of a partially saturated mixture of 70 percent bentonite and 30 percent quartz sand. Along the inner and outer radii of the buffer material lie thin layers of quartz sand in which water can be injected to simulate flow into the system through a fracture or seepage from the surface of a borehole. Sensors are installed to monitor temperature, heat flux, water content, displacement, swelling pressure, and stress within the buffer material as well as other components of the engineered barrier system. The experiment consists of uniform water injection along the outer edge of the buffer material as well as heating of the canister. The main objective was to evaluate the heat transfer and water uptake behavior of the engineered barrier system under the THM coupling conditions.

The finite element code ABAQUS with the option of two types of discrete joint elements was used to analyze the TC3 problem, primarily because it has the capability to model fluid flow under partially saturated conditions including fracture flow as well as swelling of materials. In analyzing the TC3 problem, two separate finite element analyses were performed using ABAQUS, namely, a heat transfer analysis followed by a poroelastic or consolidation analysis. These dual analyses were necessary since ABAQUS does not have elements capable of incorporating all three coupling mechanisms. Identical finite element meshes were used for the two analyses, such that the node numbers were the same in both models. However, heat transfer elements were used in the first analysis, while stress/displacement elements with pore pressure were used in the second analysis. At specified times during the thermal analysis, nodal temperatures were printed to a file. These nodal temperatures were then read in during the consolidation analysis to calculate the thermal-induced expansion within the engineered barrier materials. For each finite element mesh, a total of 1,455 elements and 5,995 nodes were used.

ABAQUS results were compared with the experimental measurements of temperature, water content, and swelling pressure within the buffer material. Comparison of temperatures shows good agreement between the numerical predictions and experimental results, considering that the thermal boundary conditions and properties of the gap material were not well defined in the problem specifications. It was found that better comparisons among temperatures were obtained by not using the properties of the gap layers given in the specifications, and assigning thermal properties equal to that of the adjacent bentonite buffer material. Fairly good agreement was found in comparisons of the water contents within the buffer at the end of the experiment (i.e., 5 months). However, ABAQUS overpredicts the water content within the innermost regions of the buffer, apparently because it cannot simulate the drying effect adjacent to the heater since ABAQUS calculates only the liquid phase. The ABAQUS results do not appear to compare favorably with the experimental results for the stresses within the bentonite. Experimental measurements of swelling pressure were obtained from pressure cells attached to the outer radius of the borehole containing the bentonite. A maximum swelling pressure in the radial direction was measured at the midheight of the heater, which is also assumed to include the thermal expansion effect of the material. The ABAQUS results, however, appear to predict tension incorrectly within this outermost portion of the bentonite. The reason for this behavior is unclear at this time. One explanation is that it may have been more appropriate to use an inelastic model versus an elastic model with swelling for the buffer. It may also be possible that the effective stress principle used by ABAQUS for unsaturated materials may need refinement. Comparison and discussion of modeling results obtained by various research teams of DECOVALEX that will be published as the DECOVALEX Phase III final report by the Swedish Nuclear Power Inspectorate may provide additional explanation on this behavior.

1 INTRODUCTION

1.1 BACKGROUND

DECOVALEX (acronym for the **DE**velopment of **CO**upled models and their **VAL**idation against **EX**periments in nuclear waste isolation) is an international cooperative project to support the development of mathematical models of coupled processes in the geosphere and their applications and validation against experiments in the field of nuclear waste isolation. The DECOVALEX project has been organized to increase the understanding of three processes, thermal-hydrological-mechanical (THM), for rock mass stability and radionuclide release and transport from a repository to the biosphere and to assess how they can be described by mathematical models. The state-of-the-art and possible directions of future research in the field of coupled processes can be found in the literature (Tsang, 1991; Manteufel et al., 1993). The DECOVALEX project was started in 1991 and included both benchmark test (BMT) and test case (TC) problems. The DECOVALEX project has three phases: Phase I, Phase II, and Phase III, each with a duration of about 1 yr. Four workshops have been held to present, discuss, and compare the preliminary and final results of DECOVALEX Phases I and II, and the preliminary results of Phase III. Phase I of DECOVALEX included the study of three problems: (i) Far-Field THM Model, BMT1; (ii) Multiple Fracture Model, BMT2; and (iii) Coupled Stress-Flow Model, TC1. Results of the Phase I study are given by Ahola et al. (1992) and Jing et al. (1993), among others. Phase II of DECOVALEX included the study of two problems: (i) Near-Field Repository Model, BMT3; and (ii) Coupled Stress-Flow Model, TC1:2. The TC problem—Coupled Stress-Flow Model, TC1:2—is a revision of the Coupled Stress-Flow Model, TC1, modeled during Phase I, with additional features and modifications to aid in overcoming some modeling problems encountered during Phase I. Results of the Phase II study are given by Ahola et al. (1993) and Jing et al. (1994), among others. A total of five TC problems were chosen for DECOVALEX Phase III: (i) Fanay-Augeres THM Experiment, TC2; (ii) Big-Ben Experiment, TC3; (iii) Triaxial Test, TC4; (iv) Direct Shear-Flow Test, TC5; and (v) Borehole Injection Test, TC6. For DECOVALEX Phase III study, the Center for Nuclear Waste Regulatory Analyses (CNWRA) research team activities include conducting experiment and preparing problem specifications for modeling by various research terms for TC5, Direct Shear-Flow Test, and modeling two problems: TC3, Big-Ben Experiment; and TC5, Direct Shear-Flow Test. This report presents the results of analysis for the Big-Ben Experiment (TC3) of the DECOVALEX Phase III study conducted by the CNWRA research team using Version 5.3 of ABAQUS (Hibbit, Karlsson and Sorensen, Inc. (1992).

1.2 DECOVALEX PROBLEMS: PHASE III

In addition to the Big-Ben Experiment (TC3) which is discussed in Section 5, the other four TC problems chosen by the DECOVALEX Steering Committee for modeling during Phase III of DECOVALEX, are briefly discussed below.

- <u>Fanay-Augeres THM Experiment (TC2)</u>—This THM field experiment was proposed and conducted by the Institut De Protection Et De Surete Nucleaire (IPSN) of France. The experiment was conducted in an underground laboratory at a depth of 100 m within the Fanay-Augeres uranium mine, France. The geological environment is a two-mica leucogranite with medium cracking. The experimental laboratory was blasted out of the rock, resulting in a square cross-section of 10x10 m, with a height of 5 m. The floor, instrumented for the experiment, comprised of a volume of granite 10x10x5-m thick served as the base of the experimental laboratory. The purpose of the experiment was to simulate on a reduced scale the THM effects provoked in a granite environment by a heat-producing radioactive waste repository. The experiment produced a large database concerning changes in temperature, and strain within the rock matrix and fractures. The absence of water led the IPSN to develop special hydraulic tests for studying the hydrological and mechanical behavior of certain cracks during heating. Detailed specifications of this problem are given by Gros (1992).

- Triaxial Test (TC4)—This experiment was proposed by the Laboratory of Rock Engineering (Helsinki University of Technology) to determine the THM-coupled behavior of a rock joint by using a digitally controlled rock mechanics testing system. The laboratory test is conducted in a triaxial cell where it is possible to apply the needed confining pressure (normal stress across the joint) and water pressure (water flow) through the joint and, at the same time, increase the temperature up to 100 °C. The triaxial test specimens containing either a natural joint or one created by splitting, are 100 mm in diameter and cored from the Kuru grey granite in Finland. The first experimental sequence consists of axial loading of the rock specimen with a joint and building up of normal stress over the joint by confining pressure. During the second sequence, water is injected through the joint under constant pressure, allowing hydromechanical equilibrium to be reached. Finally, in the third sequence, the system is heated to 90 °C while, at the same time, injecting water into the joint, allowing the system to reach a new state of hydromechanical equilibrium. Measurements are made of normal and shear stresses and strains along the joint, axial stress, water pressure, flow rates, and temperatures. The specifications of this problem are given by Laboratory of Rock Engineering (1993).

- Direct Shear-Flow Test (TC5)—This experiment was proposed by the CNWRA to study the hydromechanical response of a natural rock joint in a welded tuff under partially saturated conditions. The experimental apparatus is capable of applying direct shear along a rock joint under constant normal loading, while at the same time injecting water into the joint. The rock matrix and joint are first saturated completely. Air is then injected such that a small but constant pressure drop is maintained between the inlet and outlet ports, with the outlet pressure being maintained at 1 atmosphere. Depending on the pressure drop, the injected air causes some water to be displaced from the fracture, creating a partially saturated state within the fracture. Relationships will be developed between the pressure as well as relative conductivity versus saturation within the fracture. The effect of normal and shear deformation along the joint on these relationships will also be established. Detailed specifications of this problem are given by Mohanty et al. (1994).

- Borehole Injection Test (TC6)—This experiment was proposed by the Royal Institute of Technology (KTH) to study the hydromechanical behavior of fractured crystalline rocks subjected to high-pressure testing between a pair of inflatable packers. Specifically, the objective of the test case is to model the hydromechanical behavior of a single horizontal fracture submitted to three different hydraulic tests—pulse, hydraulic jacking, and constant pressure testing. The three tests were conducted at pressures that exceeded the overburden pressure of the rock in place. The fracture considered in Test Case 6 is located at a depth of 356 m and the *in situ* normal stresses across the fracture are estimated at 10.2 MPa (DECOVALEX, 1993a).

1.3 COMPUTER PROGRAMS FOR THM PROCESSES

Currently, few codes are capable of solving coupled three-dimensional (3D) THM problems in fractured rock masses (Manteufel et al., 1993; Kana et al., 1991). Some of the two-dimensional (2D) and 3D computer programs with various degrees of THM-coupled modeling capabilities being used or considered by DECOVALEX research teams from several countries include ROCMAS II (Noorishad and Tsang, 1989), ABAQUS (Hibbitt, Karlsson, & Sorensen, 1992), THAMES 3D (Ohnishi et al., 1985), UDEC (Board, 1989a), FLAC (Board, 1989b), MOTIF (Jing et al., 1993), CASTEM-2000 (Ababou et al., 1993), and the three code set of VIPLEF, CHEF, and HYDREF (Tijani, 1991). The CNWRA research team has selected ABAQUS for DECOVALEX Phase III. The selection of ABAQUS is based on the findings of the evaluation of computer codes for compliance determination (Ghosh et al., 1994).

1.4 OBJECTIVE AND STRUCTURE OF THE REPORT

This report presents a THM-coupled analysis by the CNWRA research team on the TC3 experiment as a part of the Phase III activities of DECOVALEX. This problem was analyzed using the finite element code ABAQUS. During Phases I and II, the CNWRA team used the distinct element code UDEC to analyze several BMT and TC problems (e.g., Ahola et al., 1992; 1993). However, all of these THM problems involved saturated hydrologic conditions. Since the focus of the U.S. radioactive waste disposal program has been on coupled THM processes in a partially saturated and fractured host rock, it was necessary to identify a code in addition to UDEC that was capable of analyzing partially saturated fluid flow through rock matrix and fractures. ABAQUS was thus chosen by the CNWRA research team for further evaluation and verification of its ability to predict THM-coupled behavior under such partially saturated conditions (Ghosh et al., 1994). As part of this evaluation, it was decided to use ABAQUS to analyze the TC3 experiment of DECOVALEX, primarily because the intent of this problem was to evaluate heat transfer and water uptake in a partially saturated buffer material surrounding a heat source. The objective of this report is to present the analysis results of the TC3 experiment.

Sections 2 and 3 give a brief description and the mathematical background of the ABAQUS code related to THM-coupled modeling, respectively. Section 4 gives a brief definition of the TC3 problem, along with the modeling approach taken by ABAQUS. Section 5 gives comments on the given specifications for the TC3 problem. Sections 6 and 7 give the results and follow-up discussion of the results, respectively. Recommendations for future modeling of the TC problem are given in Section 8. Finally, the summary and conclusions are discussed in Section 9.

2 BRIEF DESCRIPTION OF THE ABAQUS CODE

ABAQUS is a general purpose, commercially available finite element code with the option of two types of discrete joint elements. ABAQUS is currently under evaluation at the CNWRA for its use in coupled THM analysis related to the underground disposal of spent nuclear fuel. The ABAQUS system includes ABAQUS/Standard, a general-purpose finite element program, and ABAQUS/Explicit, an explicit dynamics finite element program. Only the ABAQUS/Standard program, which, for simplicity, is called ABAQUS throughout the remainder of this report, is under evaluation and was used in modeling the TC3 problem.

ABAQUS provides the capability to model heat transfer problems as well as problems involving coupled thermal-mechanical behavior. For a coupled thermal-mechanical analysis, the user has two options. The user may first run the thermal analysis, storing nodal temperatures at various time increments. A separate mechanical analysis can then be run in which, as time progresses, the nodal temperatures are read into the mechanical analysis and thermally induced strains are computed. The second option allows the user to run a fully coupled thermal-mechanical analysis.

ABAQUS also provides capabilities for modeling coupled pore fluid diffusion/stress analysis problems involving partially or fully saturated fluid flow including fracture flow. The mechanical part of the model is based on the effective stress principle. The model also uses a continuity equation for the mass of wetting fluid in a unit volume of the medium. This equation is written with pore pressure (the average pressure in the wetting fluid at a point in the porous medium) as the basic variable. ABAQUS can not track the nonwetting fluid (which in most cases is air). The code assumes that the pressure applied to the nonwetting fluid is constant throughout the domain being modeled, does not vary with time, and is small enough that its value can be neglected. This assumption requires that the nonwetting fluid can diffuse through the medium sufficiently freely so that its pressure never exceeds the pressure applied to this fluid at the boundaries of the medium, which remains constant throughout the process being modeled. Partially saturated fluid flow or consolidation problems are usually transient as well as nonlinear in nature. For such problems, ABAQUS uses the standard Newton or quasi-Newton schemes to solve the nonlinear coupled diffusion/stress analysis problem. ABAQUS also contains a large number of material models to simulate, for instance, the swelling behavior of unsaturated materials due to changes in moisture content.

Direct coupling among thermal, mechanical, and hydrologic processes is not allowed in ABAQUS. In other words, the code does not contain element types with displacement, pore pressure, and temperature degrees of freedom. Such problems are usually solved by first running the thermal analysis, and storing the nodal temperatures at different intervals in time. The hydro-mechanical analysis is then run using the same mesh. The file containing the nodal temperatures is then periodically read into the hydro-mechanical analysis to compute the thermally induced stresses, buoyant forces, etc. This process was used in analyzing the TC3 problem. Section 3 summarizes mathematical aspects of those ABAQUS features and modules used in analyzing the TC3 problem.

3 MATHEMATICAL BACKGROUND OF THE ABAQUS CODE

The following two subsections discuss briefly those mathematical models and pertinent equations in ABAQUS that were utilized in the analysis of the TC3 experiment. These models are the uncoupled heat transfer, and coupled pore fluid diffusion and stress analysis models. Detailed information on these and other available models, application of the code, and detailed theoretical background are given in the ABAQUS Manuals (Hibbitt, Karlsson, & Sorensen, Inc. 1992).

3.1 THERMAL ANALYSIS

ABAQUS has the capability to model fully coupled temperature-displacement as well as straight uncoupled heat transfer analyses. A pure heat transfer analysis, as was done for the TC3 experiment, is intended to model solid body heat conduction with temperature-dependent conductivity as well as general convection, temperature, and radiation boundary conditions. The general energy equation is solved assuming that heat conduction is governed by the Fourier law:

$$f = -k\frac{\partial \theta}{\partial x} \quad (3\text{-}1)$$

where

k = temperature-dependent thermal conductivity (W/m-°C)
f = heat flux (W/m^2)
x = position (m)
θ = temperature (°C)

The thermal conductivity may be fully anisotropic, orthotopic, or isotropic.

3.2 COUPLED PORE FLUID DIFFUSION AND STRESS ANALYSIS

The porous medium theory used in ABAQUS is based on the conventional effective stress principle, with compressibility of the solid and fluid phases allowed in the continuity equation. The porous medium modeling provided in ABAQUS considers the presence of two fluids in the medium, usually water and air. Both fluids can have some degree of compressibility. The governing equations for pore fluid diffusion/deformation are the equilibrium equation as well as the continuity equation for the wetting liquid phase in a porous medium.

The total stress acting at a point, σ_T, is assumed to be made up of an average stress in the wetting liquid, u_w, called the wetting liquid pressure, and average stress in the other fluid, u_a, and an effective stress, σ^*, defined by

$$\sigma^* = \sigma_T + \left[\chi u_w + (1 - \chi) u_a\right] \quad (3\text{-}2)$$

In Eq. (3-2), tensile stresses are assumed to be positive whereas suction in the wetting fluid in considered negative. The factor χ depends on the saturation and on the surface tension of the solid/liquid system, being equal to 1.0 when the medium is fully saturated and between 0.0 and 1.0 in unsaturated systems, when its value depends on the degree of saturation of the medium. For simplicity, ABAQUS assumes that χ is equal to the saturation of the medium, thus neglecting surface tension effects. Also, the model is simplified by assuming that the pressure applied to the nonwetting fluid is constant throughout the domain being modeled, does not vary with time, and is small enough that its value can be neglected. Thus, the form of Eq. 3-2 implemented in ABAQUS reduces to

$$\sigma^* = \sigma_T + \chi u_w \tag{3-3}$$

Fluid flow through the material is assumed to be governed by Darcy's law, where the permeability may depend on the void ratio. Darcy's law states that, under uniform conditions and low flow velocities, the volumetric flow rate of the wetting liquid through a unit area of the medium, snv_w, is proportional to the gradient of the piezometric head:

$$snv_w = \hat{k} \cdot \frac{\partial \phi}{\partial x} \tag{3-4}$$

where ϕ is the piezometric head, defined as

$$\phi = z + \frac{u_w}{g \rho_w} \tag{3-5}$$

and

s = saturation
n = porosity
v_w = velocity of the wetting fluid (m/s)
z = elevation above some datum (m)
g = gravitational acceleration (m/s^2)
ρ_w = density of water (kg/m^3), and
$\hat{k}$ = permeability of the medium (m/s)

The permeability of a particular fluid in a multiphase flow system depends on the saturation of the phase being considered and on the porosity of the medium. In ABAQUS, these dependencies are assumed separable, so that

$$\hat{k} = k_s k(x,e) \tag{3-6}$$

where $k_s(s)$ provides the dependency on saturation, with $k_s(1) = 1$, and $k(x,e)$ is the permeability of the fully saturated medium, where e is the void ratio.

For analysis involving partially saturated flow conditions, ABAQUS contains a material model for moisture swelling that defines the saturation-driven volumetric swelling of the solid skeleton. The model assumes that the volumetric swelling of the solid skeleton is a function of the saturation of the wetting fluid. The swelling is assumed reversible. The swelling strain is calculated with reference to the initial saturation so that

$$\epsilon_{ii}^{ms} = r_{ii} \frac{1}{3} \left[\epsilon^{ms}(s) - \epsilon^{ms}(s^{I}) \right] \qquad (3\text{-}7)$$

where

$\epsilon^{ms}(S)$	= volumetric swelling strain at current saturation
$\epsilon^{ms}(S^{I})$	= volumetric swelling strain at initial saturation
r_{ii}	= anisotropic swelling ratios (i = 1, 2, or 3)

4 BIG-BEN EXPERIMENT

4.1 BRIEF DESCRIPTION OF THE PROBLEM

The Big-Ben Experiment was designed to evaluate the engineered barrier system for the current Japanese radioactive waste disposal concept as shown in Figure 4-1. It is composed of an electric heater, carbon steel overpack, buffer material, and concrete containment simulating the surrounding host rock. The reinforced concrete containment for the experiment has an outside diameter of 6 m and is 5 m in height. A borehole approximately 1.7 m in diameter and 4.5 m in depth, is located in the center of the concrete. An electric heater with several cartridge heaters is set in the overpack, which is about 1 m in diameter and about 2 m in height. Figure 4-1 shows the types and locations of measurements taken throughout the experiment. This particular experiment consisted of uniform heating as well as vertical water injection under constant pressure through a tube from the surface of the borehole as depicted in Figure 4-1. The uniform heating and water injection were carried out for a period of 5 months during which time periodic measurements of temperatures, strains, water contents, swelling pressures, etc. were taken.

Figure 4-2 shows a closeup view of the buffer material region. The buffer itself is composed of a mixture of 70 percent bentonite and 30 percent quartz sand. It is partially saturated, having an initial saturation of approximately 0.63 (i.e., 63 percent). Around the inner and outer edges of the bentonite lie two thin, highly permeable quartz sand layers a few centimeters in thickness. During the experiment, water is injected through a tube directly into the outer quartz sand layer at a constant pressure of 50 kPa throughout the 5-month period to simulate water flowing in from the surface of the borehole through a fracture. Over this same 5-month period, the heater was operated at a constant power output of 0.8 kW. The THM coupling effects thus consisted of water being imbibed into the buffer material, creating an increase in saturation and swelling of the material. In addition, the heating was causing thermal expansion within the different materials, in addition to forcing moisture outward and thus desaturating the inner portions of the buffer material. Further specifications of this problem are given in DECOVALEX (1993b).

4.2 DEFINITION OF INPUT PARAMETERS

The properties of the bentonite are given in Table 4-1. The initial water content (ω_0) for the bentonite was established at 0.165, corresponding to a volumetric water content (θ_0) of 0.264. Based on the specified initial porosity n_0 of 0.41, the theoretical saturated water content is determined to be 0.265, corresponding to a volumetric water content of 0.41. As shown in Table 4-1, the Young's modulus and uniaxial compressive strength of the bentonite were determined experimentally to decrease rather significantly with increasing water content. Likewise, changes in temperature were found to have much less effect on the thermal properties (i.e., thermal conductivity and specific heat) than changes in water content within the bentonite.

For modeling the partially saturated flow within the bentonite with ABAQUS, additional relationships are needed between the pressure (i.e., suction) versus saturation, as well as the relative conductivity versus saturation. Such relationships are usually nonlinear in nature, with the extent of the nonlinearity depending on certain characteristics of the material. One such set of relationships that have been found to fit well to a wide range of soil materials was developed by van Genuchten (see for example Ababou, 1991). These relationships can be written as follows:

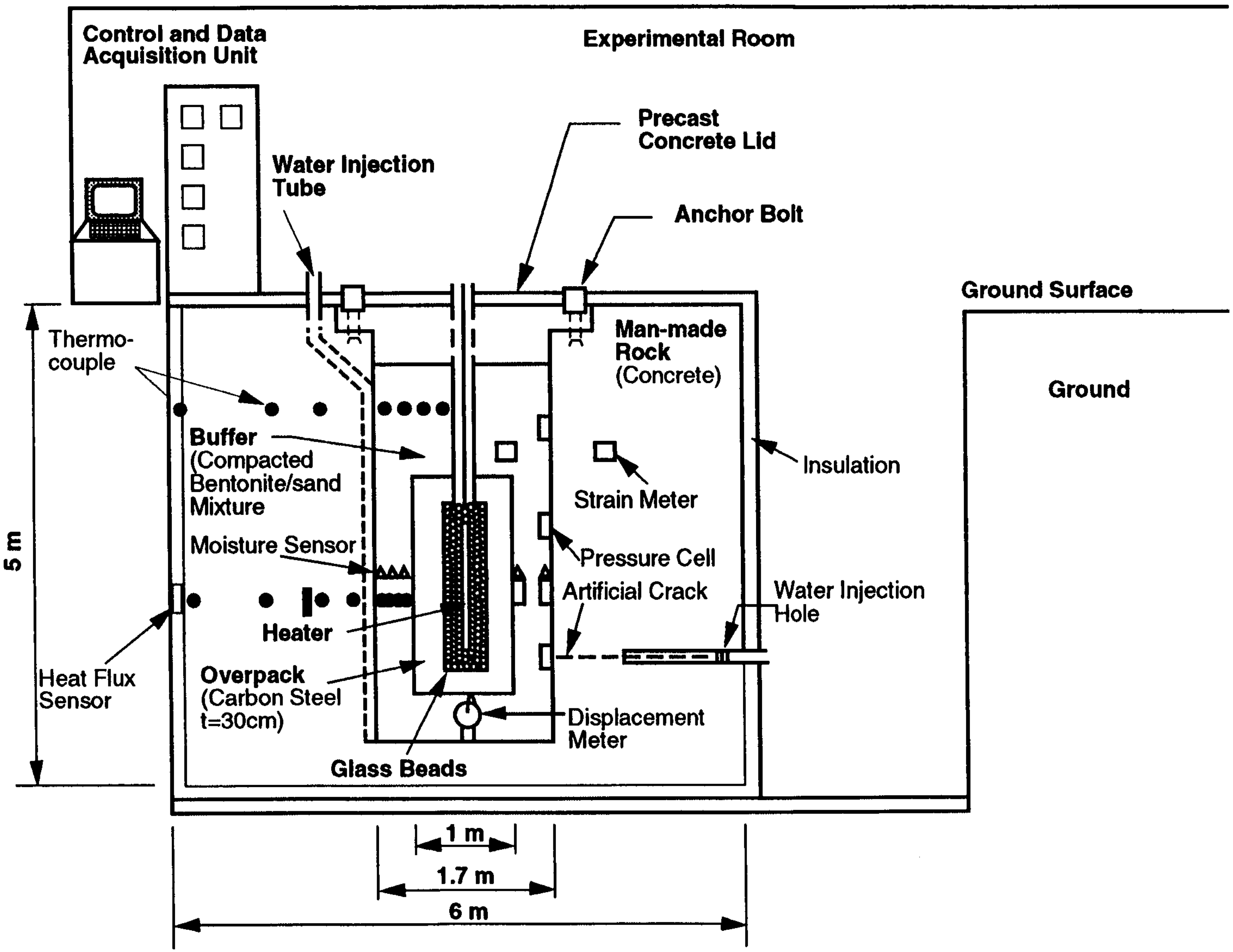

Figure 4-1. Schematic view of Big-Ben experiment equipment

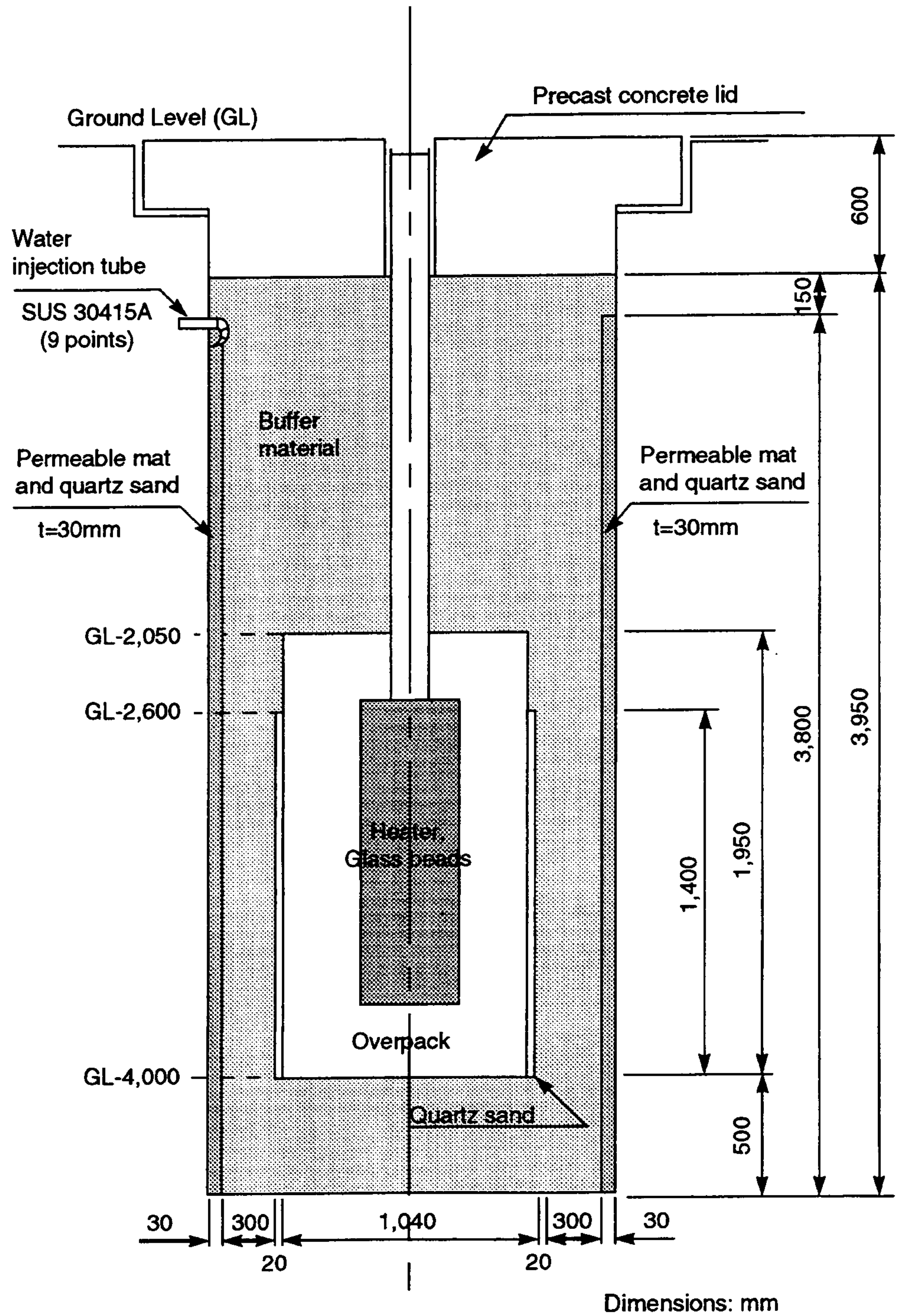

Figure 4-2. Schematic view of Big-Ben experiment equipment (buffer material)

Table 4-1. Properties of buffer material composed of a 70-percent bentonite and 30-percent quartz sand mixture compacted to a dry density of 1.6 g/cm^3

Property	Value	
Initial wet density ρ_t [g/cm^3]	1.86	
Initial dry density ρ_d [g/cm^3]	1.6	
Initial water content ω_o	0.165±0.01	
Initial porosity n_0	0.41	
Young's modulus E [MPa]	27 (ω=0.168)	10 (ω=0.259)
Uniaxial compressive strength σ_c [MPa]	15 (ω=0.168)	6.8 (ω=0.259)
Saturated permeability K [m/s]	4.0E-13	
Thermal conductivity K_t [W/m -°K]	0.33+3.1θ	
Specific heat C [kJ/kg -°K]	(1 + 4.2 ω)/(1 + ω)	
Thermal expansion [1/°C]	1.0E-4	
Density of water; ρ_w [g/cm^3] Volumetric water content; $\theta = \omega\rho_d/\rho_w$		

$$S = (S_s - S_r)\left[\frac{1}{1 + |\alpha\psi|^\beta}\right]^{\left(1 - \frac{1}{\beta}\right)} + S_r \tag{4-1}$$

and

$$K_r = \sqrt{S_e}\left\{1 - \left[1 - (S_e)^{\frac{1}{\lambda}}\right]^\lambda\right\}^2 \tag{4-2}$$

where

α, β = van Genuchten fitting constants

λ = $1 - \dfrac{1}{\beta}$

ψ = pressure or suction (MPa)

S = saturation

S_s = saturation at full saturation = 1.0 (maximum obtainable saturation)

S_r = residual saturation (minimum obtainable saturation)
K_r = relative conductivity

S_e = effective saturation $\left[S_e = \dfrac{S - S_r}{S_s - S_r} \right]$

Eq. (4–1) is van Genuchten's model for saturation in terms of suction pressure while Eq. (4–2) is a combination of Mualem's model for relative permeability in terms of both saturation (S) and suction (ψ) with van Genuchten's model (Green et al., 1993). Although Eqs. (4-1) and (4-2) contain three unknown constants, only two are independent of each other (i.e., α and β). As a result, once the suction pressure versus saturation data are fit to the van Genuchten relationship (Eq. 4-1), the relative conductivity versus saturation is given automatically by Eq. (4-2) using the relationship between β and λ. Since the specifications for the TC3 problem provided only experimental data relating the suction pressure and saturation within the bentonite, it was decided to fit the available data to a van Genuchten relationship. Figure 4-3 shows the experimental data provided for the pressure versus saturation relationship for the bentonite/quartz sand mixture, and corresponding van Genuchten fit. The actual experimental data provided only volumetric water contents, and did not give any value for the residual water content (θ_r) of the bentonite. Thus, in order to determine the residual saturation for use in the van Genuchten relationships, a value for the residual water content was extrapolated from the data provided. This value for the residual water content was chosen to be 0.02. Figure 4-3 shows that the van Genuchten relationship fits the data well over values of saturation ranging from 0.30 to 0.85. However, at the extreme low and high values of saturation, there is considerable deviation from the experimental results provided. It is not clear why there is such an abrupt change in slope in the experimental data at the very high saturation end. It was determined that the fitted van Genuchten relation was acceptable since the initial starting saturation for the bentonite was approximately 0.626. During the later stage of the TC3 experiment, the outermost portion of the bentonite ring would approach saturation, leading to some error in using the fitted van Genuchten relation versus the actual hydrologic response. The values for the two fitting parameters α and β from the van Genuchten fit were determined to be 0.079 1/MPa and 2.0785, respectively. Figure 4-4 shows the relation between the relative conductivity and saturation, easily obtained once the fitting parameters in the van Genuchten relation are determined. The relative conductivity is defined as the unsaturated hydraulic conductivity divided by the saturated hydraulic conductivity, and thus approaches one as the saturation approaches one.

Data specified for the swelling characteristics of the bentonite gave only the swelling pressure as a function of time. These data were not used for the ABAQUS analysis since they gave no indication of how the pressure or volumetric strain varied with saturation. As input, ABAQUS requires a table giving the swelling ratio as a function of saturation. The swelling ratio (ε), defined as the change in volume over the initial volume, is also considered to depend on the initial compacted dry density, confining pressure or surcharge, and temperature. However, these dependencies are not accounted for in the ABAQUS analysis. Following the approach taken by Fujita et al., 1991, a linear relationship was assumed between the swelling ratio and degree of saturation, that is, $\left[\varepsilon = \gamma(S - S_o) \right]$ where γ is the swelling coefficient and S_o is the initial saturation. However, in that report the buffer was composed of 100-percent bentonite whereas in the TC3 experiment, a mixture of 70 percent bentonite and 30 percent quartz sand was used. The corresponding maximum swelling pressure for this mixture was approximately one-seventh that of 100 percent bentonite. Thus, it was decided to use one-seventh the value of the swelling coefficient obtained by Fujita et al., 1991 in generating the tabular moisture swelling data for the ABAQUS analysis.

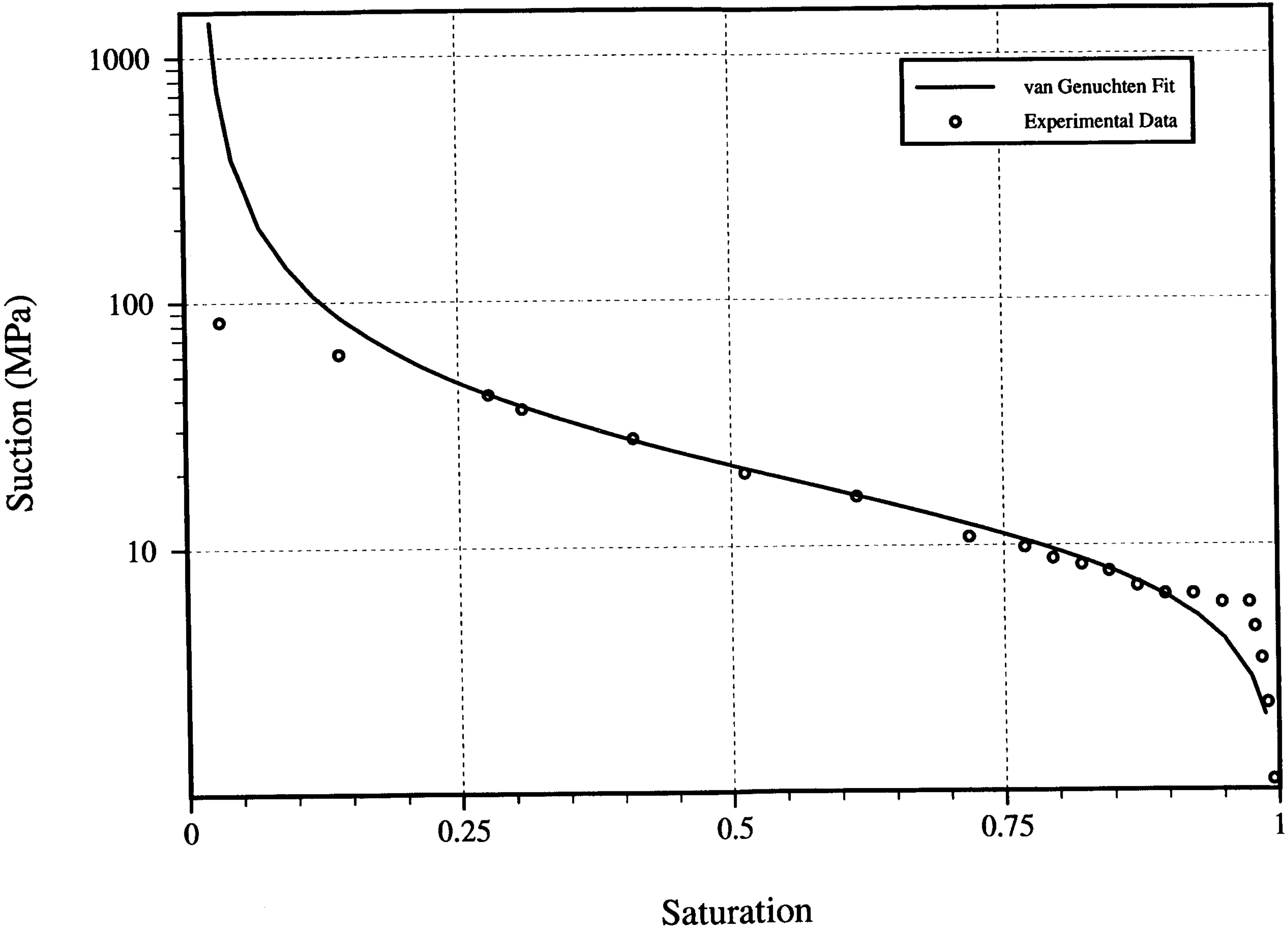

Figure 4-3. Moisture retention curve used by ABAQUS for the bentonite as determined from fitting experimental data to the van Genuchten relationship (α = 0.079 1/MPa, β = 2.0785)

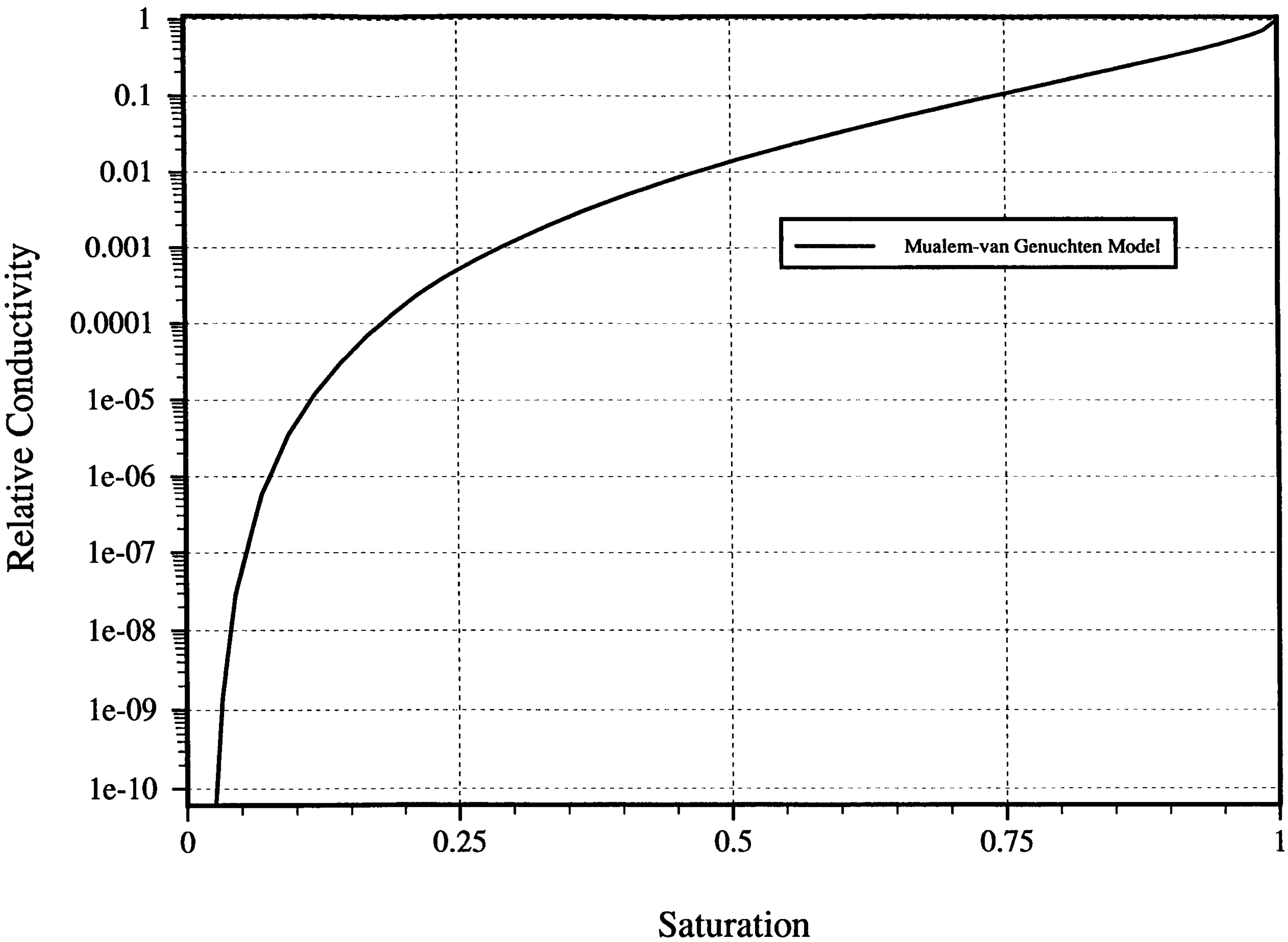

Figure 4-4. Relationship between relative conductivity and saturation used by ABAQUS for the bentonite as determined from the Mualem–van Genuchten relationships

Table 4-2 gives the mechanical, hydrologic, and thermal properties used for the remaining materials in the TC3 experiment. These materials include the glass beads, carbon steel overpack, gap layer, and concrete. As seen in the table, several of the parameters specified for the different materials range over several orders of magnitude.

Table 4-2. Input parameters used in the analysis

Parameters	Concrete	Overpack	Glass beads	Gap layer
Young's modulus [MPa]	2.50×10^4	2.0×10^5	8.2×10^4	8.30×10^{-2}
Poisson's ratio	0.167	0.3	0.3	0.45
Density [kg/m^3]	2300.0	7800.0	1600.0	1.0
Hydraulic conductivity [m/s]	1.0×10^{-14}	—	2.5×10^{-4}	3.3×10^{-1}
Specific heat [J/kg-°C]	750.0	460.0	840.0	1000.0
Thermal conductivity [W/m-°C]	1.88	5.3×10^1	2.55×10^{-1}	7.29×10^{-2}
Coefficient of thermal expansion [/°C]	1.0×10^{-5}	1.64×10^{-6}	1.0×10^{-5}	3.6×10^{-3}

4.3 ABAQUS MODELING APPROACH

A 2D axisymmetric model was used to analyze the TC3 experiment. ABAQUS does not have the capability to model all three THM processes at once. In other words, the code does not have an element with temperature, pore pressure, radial displacement, and vertical displacement degrees of freedom, inclusively. As a result, two separate analyses were conducted. The first ABAQUS analysis was a pure heat transfer analysis for the TC3 engineered barrier system. For this analysis, 8-noded quadilateral elements were used, each having temperature degree of freedom at the nodes. Figure 4-5 shows the axisymmetric finite element mesh used for the heat transfer analysis, consisting of 1,485 elements and 4,620 nodes. The elements representing the heat source are given a volumetric heat flux corresponding to a total power output from the heater of 0.8 kW. An initial temperature of 15 °C was specified for the entire model. As boundary conditions, the top, right, and lower boundaries were specified convective heat transfer boundary conditions, with the film coefficient (h) approximated at 0.5 W/m^2–°C. This is a fairly low value, which was meant to take into account some resistance to heat flow out of the concrete due to the thin layer of insulation surrounding the apparatus (see Figure 4–1). The ambient air temperature was assumed to be constant at 15 °C. Nodal temperatures were saved to a file at periodic increments (approximately every 10 days) throughout the 5-month period of analysis. The nodal temperatures were later read into the poroelastic analysis. The first runs were made assigning the thermal properties to the

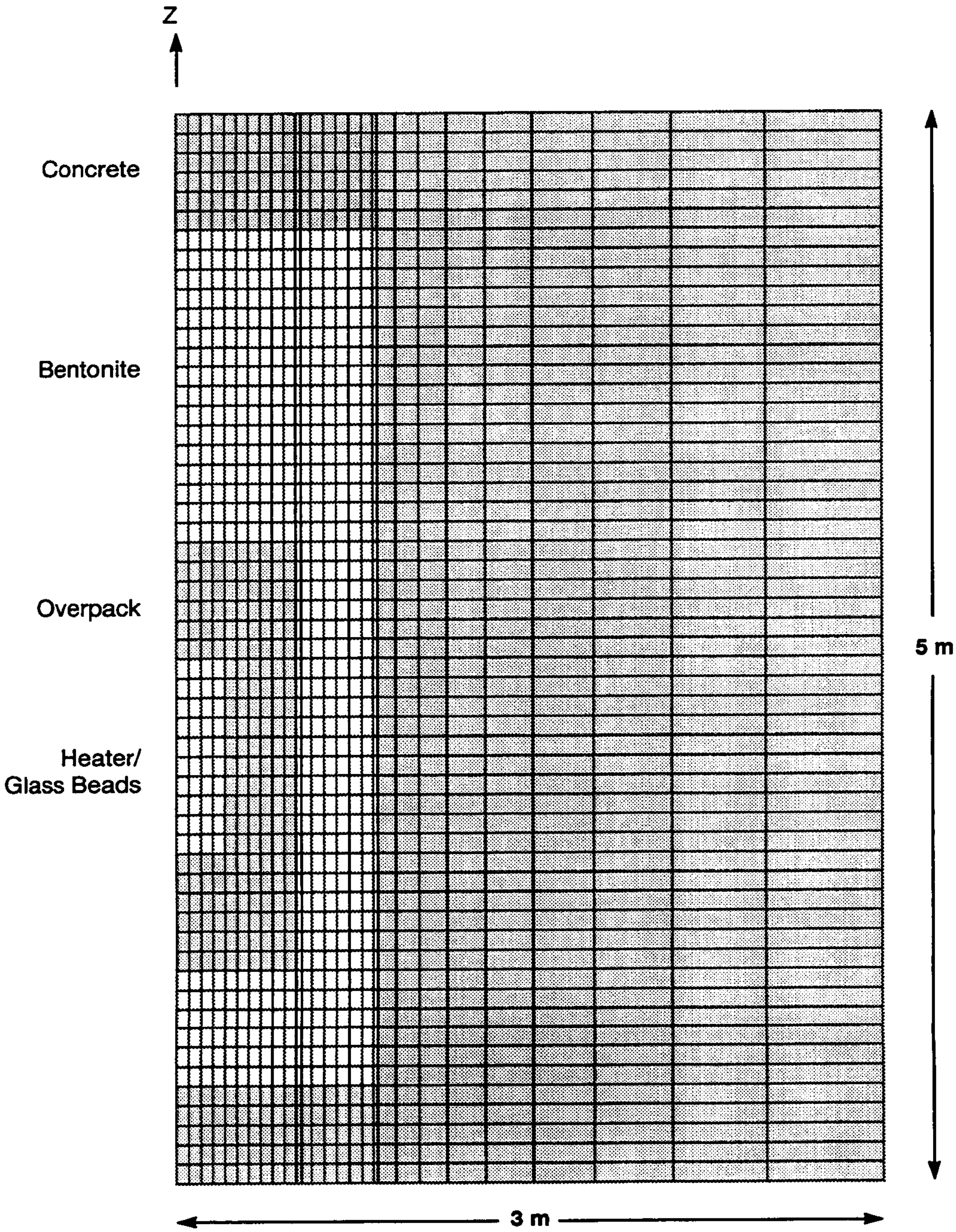

Figured 4-5. ABAQUS axisymmetric finite element mesh

gap elements as listed in Table 4-2. However, upon comparing the resulting temperatures computed from ABAQUS with the experimentally measured temperatures, it was found that fairly substantial disagreement existed. The specified low thermal conductivity value for the gap resulted in steep temperature gradients across these two thin regions that were not as evident in the actual TC3 experiment. As a result, it was decided to increase the values of the gap thermal properties to those of the surrounding bentonite. As it will be discussed in Section 6 of this report, much better correlation was found between the experimental and predicted temperature field.

For the poroelastic or coupled stress/fluid diffusion analysis, an identical mesh with the same number of nodes and node numbers was utilized. The only difference was that 8-noded quadrilateral elements having displacement and pore pressure degrees of freedom were utilized in place of the heat transfer elements. For these elements, displacement degrees of freedom were allowed at all 8 nodes, whereas pore pressure degrees of freedom were allowed only at the corner nodes. The overpack, however, was assumed to be impermeable, and thus the elements making up the overpack and glass bead/heater assembly were designated as regular solid elements without pore pressure. As discussed in the previous section, the bentonite was initially compacted in a partially saturated state, and would behave according to the derived van Genuchten relationship. The surrounding concrete was modeled as being in a fully saturated state. The fluid pressure was fixed at zero along the outer boundaries of the ABAQUS model. Similarly, the displacement along the lower boundary was fixed in the vertical direction, while zero stress or force was maintained along the top and side boundaries.

In the actual experiment, water was injected in the outer gap through a single tube and maintained at a constant 50 kPa throughout the experiment. Since the gap material was much more permeable than either the surrounding bentonite or concrete, it could be assumed that this constant pressure existed over the entire length of the gap, neglecting any additional gravity-induced pressure due to the small height involved. Thus, in the ABAQUS model, nodal pressures were fixed to 50 kPa along one side of the gap throughout the analysis. Numerous attempts were made to utilize the mechanical properties as specified in Table 4-2 for the gap layers. However, even using a more representative density, it was not possible to maintain such a low value for the Young's modulus. The initial Young's modulus of the bentonite was 27.0 MPa compared to 2.5×10^4 MPa for the concrete. Thus, a variation of three orders of magnitude in stiffness exists without taking into account the low value specified for the gap material. It would seem reasonable that the stiffness of the permeable mat and quartz sand would be somewhat comparable to that of the bentonite. Setting the Young's modulus much below that of the bentonite resulted in numerical instability problems in the ABAQUS analysis. In order to eliminate this problem, the gap layers were assigned the same elastic properties as the adjacent bentonite.

During various time increments of the poroelastic analysis, temperatures at the nodes were read in from the results file saved during the heat transfer analysis. ABAQUS performs a linear interpolation between saved states during the heat transfer analysis to update temperatures at the nodes during the consolidation analysis. Based on the changing nodal temperatures, thermally induced stresses and displacements as a result of thermal expansion are calculated at each element. The thermal expansion of the solid matrix as well as the fluid is computed based on the difference between the temperature at a particular time and the initial temperature, which in this case was 15 °C.

An additional limitation with ABAQUS in not being able to conduct a fully coupled thermal-mechanical-hydrologic analysis is that it is difficult to incorporate material property dependence on parameters other than temperature. The dependence of properties such as the thermal conductivity and Young's modulus on temperature can easily be incorporated as a table within an ABAQUS analysis.

However, there is no such provision for inputting such tabular data regarding variation with some other parameters. In the case of the TC3 experiment, the Young's modulus, thermal conductivity, and specific heat of the bentonite do not vary significantly with temperature; however, they vary fairly significantly with saturation or water content. As a result of the difficulty in accounting for these material properties variations, especially when the saturation was nonuniform throughout the bentonite, no account was taken for the effect of saturation on material properties in this analysis.

4.4 COMPUTER HARDWARE AND TIME REQUIREMENTS

The analysis of this TC3 problem was run on a Silicon Graphics ONYX Reality Engine 2 with multiprocessing capabilities. The analysis was conducted using Version 5.3-1 of ABAQUS. As discussed in the previous section, the ABAQUS analysis of TC3 was conducted in two parts, namely, a heat transfer analysis followed by a poroelastic or coupled stress/diffusion analysis. The heat transfer analysis took approximately 1.2 hr of computer run time. The poroelastic analysis took approximately 6.3 hr of computer run time. ABAQUS input data files for both the thermal and poroelastic analyses are given in Appendices A and B, respectively.

5 COMMENTS ON THE GIVEN SPECIFICATIONS FOR THE TC3 PROBLEM

A number of comments arose during detailed review of the specifications given for modeling the TC3 experiment as well as during the modeling of the experiment.

- The thermal boundary conditions were not clearly stated in the specifications. They were stated as only being heat transfer boundary conditions. After further clarification with the Japanese research team responsible for developing the specifications, the boundary conditions were later specified to be fixed at the constant temperature of 15 °C, which was the initial temperature of the experiment. However, utilization of constant temperature boundary conditions still does not appear appropriate, since the experimental data clearly show a rising temperature along the outer boundary of the experiment in time. There appears to be some thermal insulation around the experiment (Figure 4-1), however, it is likely that applying purely adiabatic boundary conditions would also not be appropriate. As a result, convective boundary conditions were assumed around the boundaries of the experiment, with the heat transfer coefficient (h) approximated to be 0.5 W/m^2-°C, based on the experimental temperature gradient through the concrete and taking the ambient air temperature to be 15 °C.

- The mechanical and thermal properties of the gap layers composed of a permeable mat and quartz sand as shown in Table 4-2 appear to be very low. For instance, the Young's modulus (E) is specified at 8.30×10^{-2} MPa with the corresponding density (ρ) specified at 1.0 kg/m^3. Setting the Young's modulus this low in the ABAQUS analysis resulted in numerical instability problems, because the modulus of the concrete was many orders of magnitude higher. As a result, the mechanical properties of the gap were set to the same values as that for the bentonite. Likewise, using the low thermal conductivity (k) specified for the gap at 7.29×10^{-2} W/m-°C, resulted in a steep temperature gradient across the gap layers that did not match well with the experimental results. Consequently, during the thermal analysis, the gap properties were assigned values representative of the bentonite. In speaking with the Japanese research team members responsible for developing the TC3 specifications, they agreed that the gap properties were not well known, and had themselves essentially neglected the effects of the gap in their numerical modeling analysis.

- The hydrologic state of the concrete was assumed to be fully saturated since only the saturated hydraulic conductivity was provided. In the ABAQUS analysis, the overpack containing the glass beads and heater was modeled using regular 8-noded solid elements (i.e., impermeable).

- No material property data were specified regarding the porous bulk moduli of the solid grains for the different materials as well as the wetting fluid. The bulk modulus of water was taken to be 2.0×10^3 MPa. The bulk modulus of the solid grains were taken from Mitchell (1976), who provided compressibility values for soil, rock, and concrete. The bulk modulus is defined as the inverse of the compressibility.

- The swelling behavior data provided for the bentonite, namely swelling pressure versus time, was not particularly meaningful in establishing input for the ABAQUS analysis. More meaningful experimental data would have provided the swelling pressure/volumetric strain with saturation or moisture content. An approximation for the volumetric swelling versus saturation was taken from Fujita et al., (1991), where they assumed a linear relationship, $\varepsilon = \gamma(S - S_o)$, where ε is the swelling ratio, S is the saturation, S_o is the initial saturation, and γ is the swelling coefficient. This work by Fujita et al. was based on the buffer material being 100 percent bentonite, in which the swelling coefficient (γ) was approximated at 0.167. In the TC3 experiment, the buffer is composed of 70 percent bentonite and 30 percent quartz sand. Consequently the linear expansive coefficient was taken to be one-seventh the value given above, since the swelling pressure as given in the specifications appeared to be roughly one-seventh that of the 100 percent bentonite buffer.

- It is assumed that the required output from the specifications for the radial and vertical stresses (Table C-1) is the effective stresses including the thermal component and the swelling stress. ABAQUS computes effective stresses. It is not clear from the specifications whether total or effective stresses were measured during the experiment.

6 RESULTS

Figure 6-1 shows the temperature distribution with radial distance at the mid-height of the heater after elapsed times of 1 and 5 months. The solid lines represent the temperatures predicted by ABAQUS, while the data points indicate experimental measurements. The figure shows good agreement among the temperatures within the buffer material and concrete. The experimental results show a temperature gradient through the overpack material which is not present in the ABAQUS results. The reason this gradient is not present in the modeling results is due to the high thermal conductivity specified for the overpack. However, it is not clear why such a gradient should exist in the actual experiment, unless the conductivity of the overpack material was more highly dependent on temperature than it was thought. It appears that temperature dependence testing of thermal properties was conducted only for the bentonite buffer material. Utilizing the thermal properties specified for the gap materials resulted in a steep temperature gradient across both the gap layers, which did not match up well with the experimental results. As a result, the thermal properties of the gap were taken to be the same as the buffer material resulting in a much better correlation. The slight discrepancies in temperatures are thus due to the inexact knowledge of the gap properties as well as the fact that ABAQUS did not account for the thermal property dependence on water content or saturation within the buffer material.

As was stated earlier, the bentonite had an initial volumetric water content (θ) of 0.264. Since the initial porosity (n) was 0.41, the saturated volumetric water content would be 0.41. During the actual experiment, the water content (ω) was measured by various means at different locations within the buffer, including using a split-spoon sampler at the end of the experiment. Figure 6-2 shows a comparison of the volumetric water content through the bentonite buffer at a depth of 1500 mm below the ground surface (i.e., level GL-1500 as shown in Figure C-1, Appendix C). The values of water content (ω) at this level were converted to values of volumetric water content (θ) using the following relation as given in the problem specifications

$$\theta = \frac{\omega \rho_d}{\rho_w} \qquad (6\text{-}1)$$

where ρ_d = initial dry density
ρ_w = density of water

The initial dry density of the packed bentonite was given as 1.6 g/cm^3 whereas the density of water can be taken as 1.0 g/cm^3. It is assumed that in converting the water content to volumetric water content, the dry density, defined as the mass of the solids over the total volume, is constant throughout the experiment. This is likely to be approximately correct since even though there is swelling of the bentonite, it is confined by the borehole wall composed of the stiffer concrete and the concrete cap held in place by anchor bolts. There is likely some expansion/swelling into the gap layers which would slightly change the dry density.

ABAQUS does not directly provide output in the form of water content. The code computes the level of saturation, varying from 0 to 1, as well as the void ratio (e) within the bentonite. The initial void ratio can be computed knowing the initial porosity (n) from the following relation

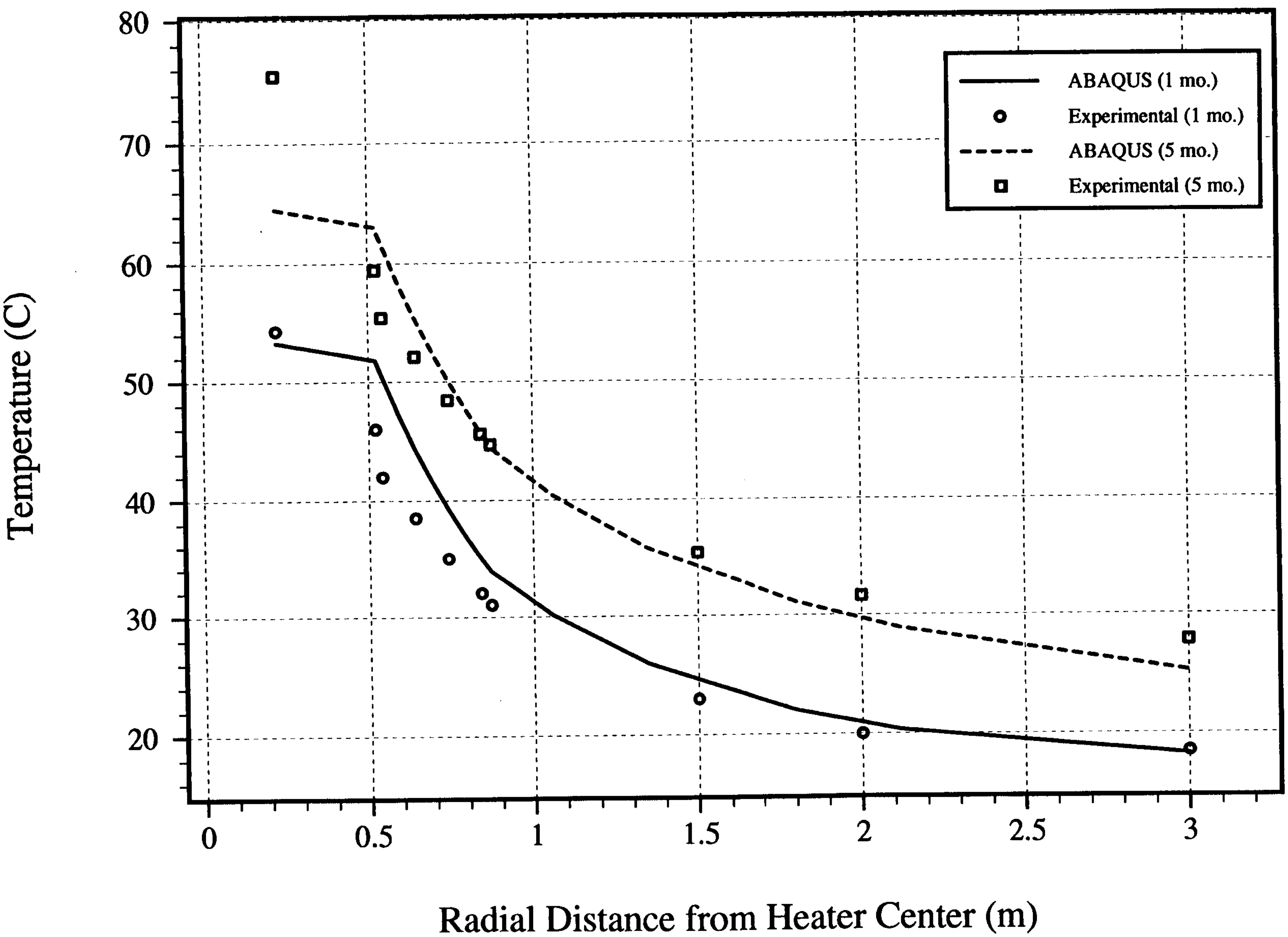

Figure 6-1. Comparison of temperatures at a depth 3,000 mm below the ground surface (GL-3000) corresponding to the mid-height of the heater

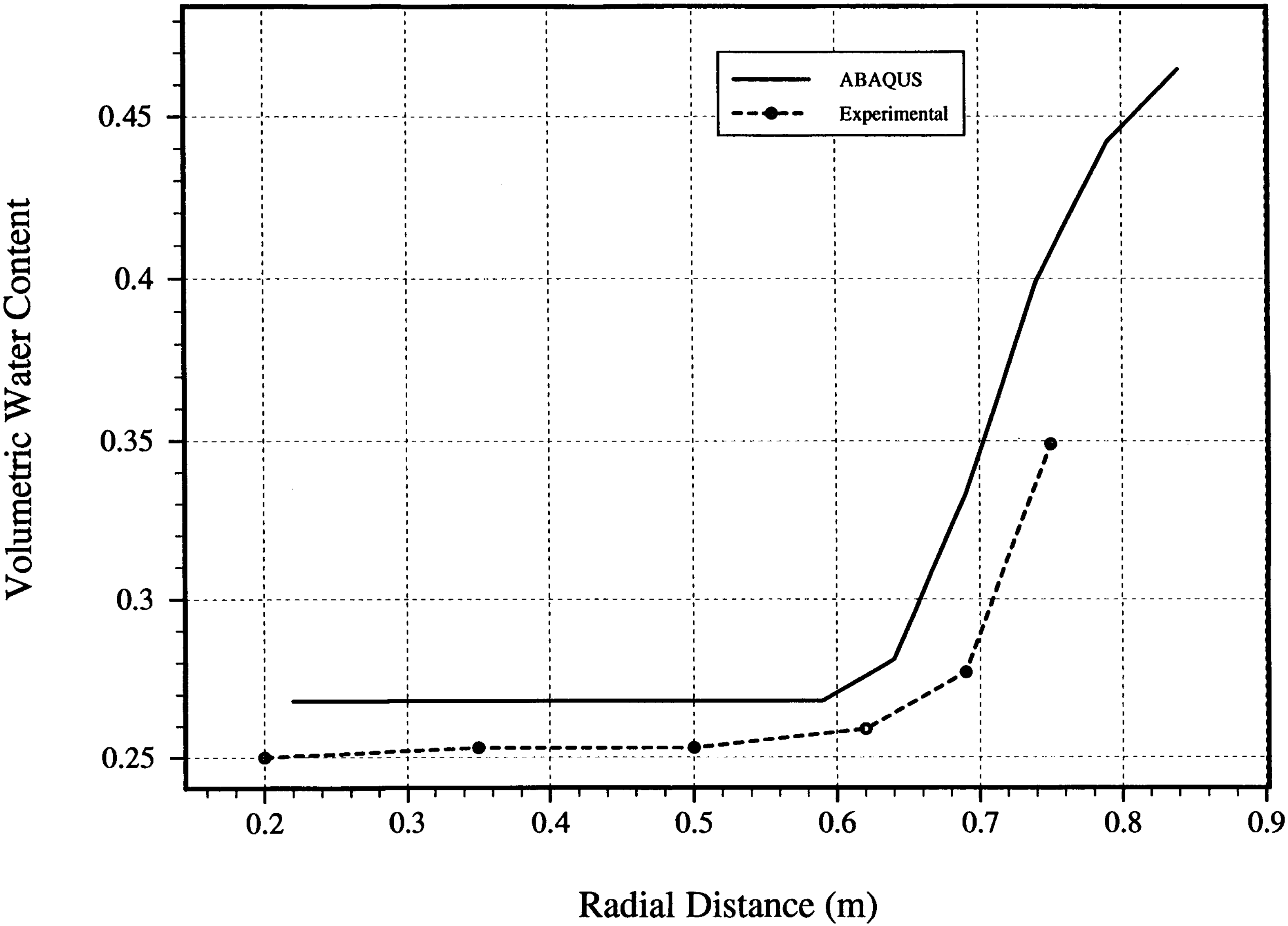

Figure 6-2. Comparison of volumetric water contents through the buffer at a depth 1,500 mm below the ground surface (GL-1500)

$$e = \frac{n}{1 - n} \qquad (6\text{-}2)$$

Since the initial porosity was given as 0.41, the initial void ratio is computed to be 0.695. The TC3 problem is complex in that the void ratio and porosity are changing with time as a result of the thermal expansion and swelling within the buffer material. As a result, the theoretical saturated volumetric water content is also changing with time. Thus, in converting the saturation given by ABAQUS into a volumetric water content, initial saturated volumetric water content cannot be used. A new relation can be developed by first noting that the volumetric water content (θ) is defined as

$$\theta = \frac{V_w}{V_T} \qquad (6\text{-}3)$$

where V_w = volume of water, and
V_T = total volume

Likewise, the porosity (n) and saturation (S) are given by the following two relations

$$n = \frac{V_v}{V_T} \qquad (6\text{-}4)$$

and

$$S = \frac{V_w}{V_v} \qquad (6\text{-}5)$$

where V_v = volume of the voids.

Solving Eq. 6-4 for V_T and substituting it into Eq. 6-3 for θ yields

$$\theta = \frac{nV_w}{V_v} = nS \qquad (6\text{-}6)$$

The above equation can be written in terms of the void ratio (e) using Eq. 6-1 as

$$\theta = \frac{eS}{1 + e} \qquad (6\text{-}7)$$

From the saturation and void ratio results calculated by ABAQUS, the above equation can be used to convert these to calculated volumetric water contents for comparison with the experimental results. As shown in Figure 6-2, ABAQUS tends to slightly overpredict the volumetric water content at the GL-1500 level, located above the heater. At the GL-2350 level (i.e., 2,350 mm below the ground surface and closer to the mid-height of the heater), ABAQUS tends to overpredict the volumetric water content only along the inner portion of the bentonite ring closer to the heat source (Figure 6-3). It is most likely that, in the experiment, the inner portion of the buffer region is being dried out due to evaporation with the moisture being driven outward away from the high temperature regions through vapor due to differences in the vapor pressure between the hotter and cooler sides of the bentonite. ABAQUS does not have the capability to track the vapor phase, and it is reasonable to expect that the corresponding volumetric water content would be higher in this inner buffer region.

Figure 6-4 shows the saturation results obtained from ABAQUS through the bentonite at the heater mid-height (i.e., GL-3000 as shown in Figure C-1, Appendix C) after 1 and 5 months, respectively. The saturation front can be seen to progress inward as time elapses. Figure 6-5 shows the corresponding plot of the void ratio taken along the same height. The void ratio is seen to decrease with time along the inner portion of the buffer material, whereas it increases with time in the outer regions. This is likely because the level of saturation and swelling is higher at the outer regions, causing an increase in void ratio.

Plots of the radial and vertical stresses through the bentonite at the mid-height of the heater (i.e., GL-3000) are shown in Figures 6-6 and 6-7. Both the radial and vertical stress components become more compressive (i.e., become more negative) with time within the inner portion of the bentonite buffer. The swelling amounts to only a few tenths of a megapascal based on the input properties provided. The remaining compressive stress is apparently due to thermal expansion. However, along the outer portion of the bentonite (i.e., near the concrete), ABAQUS predicts tensile stresses. This appears to be incorrect and apparently due to the higher suction pressures along the inner regions of the bentonite in combination with the low stiffness of the bentonite. It would be more conceivable to assume that the larger increase in saturation and subsequent increase in swelling pressure in the outer buffer region would result in compression. In the actual experiment, pressure cells were attached to the wall of the borehole at the outermost portion of the buffer material. Experimental results show the maximum swelling pressure is obtained from the pressure cell mounted to the borehole wall at the mid-height of the heater. After 5 months, this swelling pressure was measured to be 0.39 MPa. It is assumed that this swelling pressure also includes any pressure generated by thermal expansion of the material. Thus, it appears that further study is necessary to determine the cause for the discrepancy between the stresses predicted by ABAQUS and those measured experimentally. During the ABAQUS analysis, the concrete remains in a fully saturated state. However, it is peculiar to note that fairly high pore pressures (on the order of 10 MPa) are generated within the concrete even though the pressure on the outer gap nodes is maintained at 50 KPa. High tensile stresses also occur in the concrete, apparently as a direct result of this. Further study is needed to determine if this is truly realistic or if there is some problem with the model specifications (e.g., specified moisture retention curve) or the solution itself.

Figure 6-8a and b show plots of the undeformed and deformed meshes, respectively, comprising the buffer region after a period of 1 month. The deformed mesh shows the bentonite being compressed adjacent to the overpack and extended next to the concrete. This generally agrees with the stress plots. The reason for this behavior is not entirely clear due to the various coupling effects taking place. It is possible that the swelling in the outer region and high suction within the inner region is deforming the mesh in this manner.

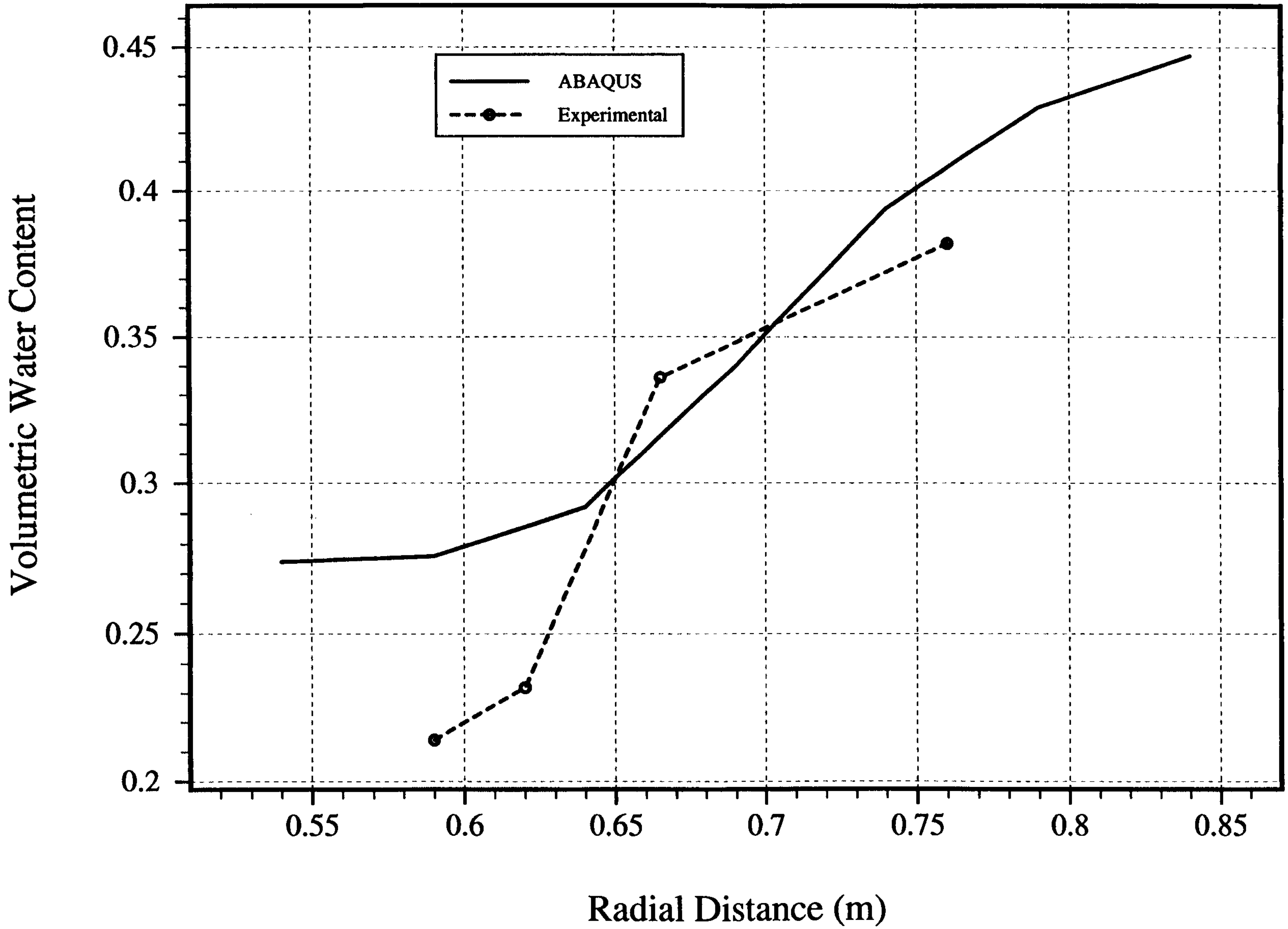

Figure 6-3. Comparison of volumetric water contents through the buffer at a depth 2,350 mm below the ground surface (GL-2350)

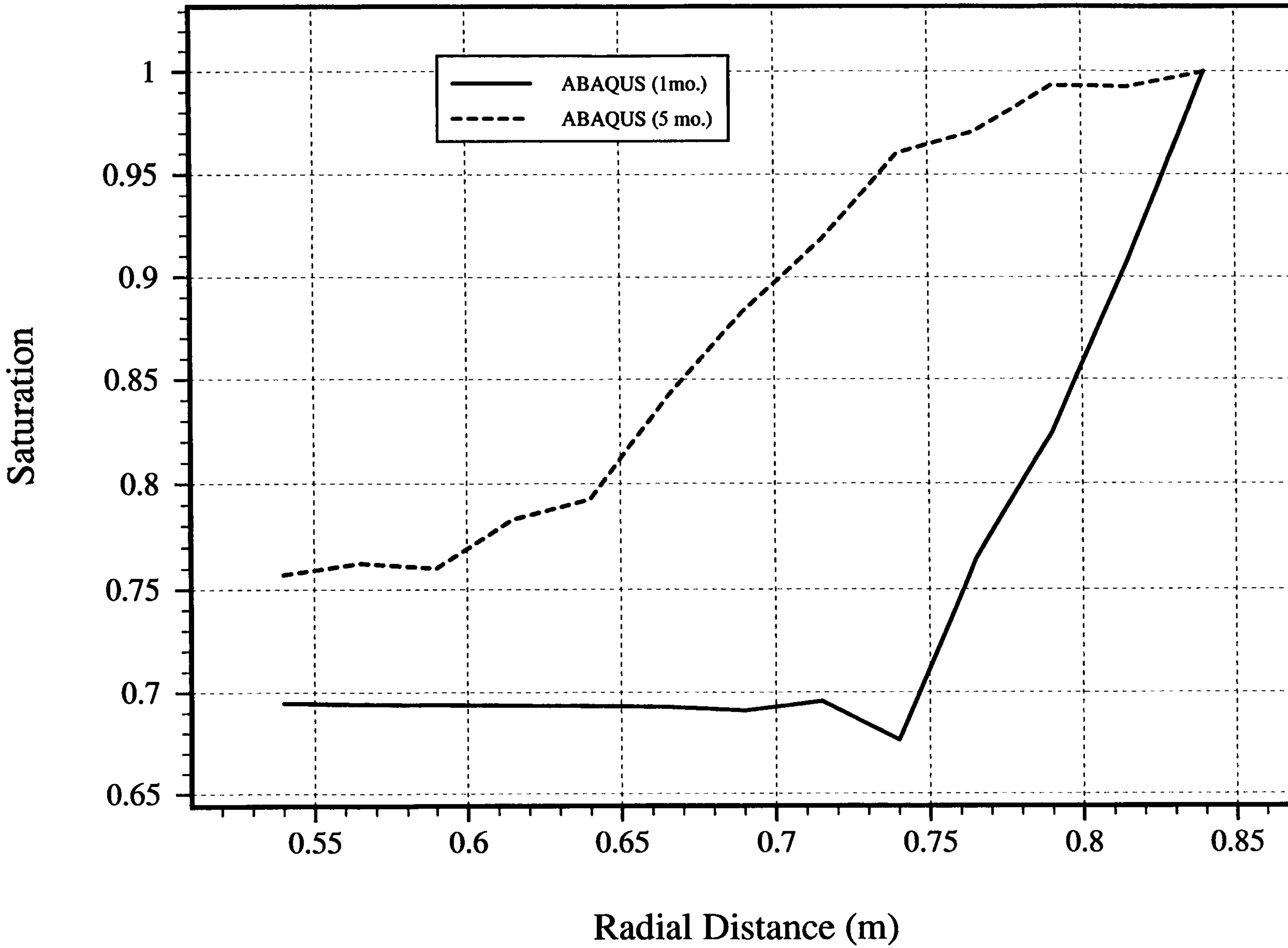

Figure 6-4. ABAQUS results for the saturation through the buffer at a depth 3,000 mm below the ground surface (GL-3000), after elapsed times of 1 and 5 months

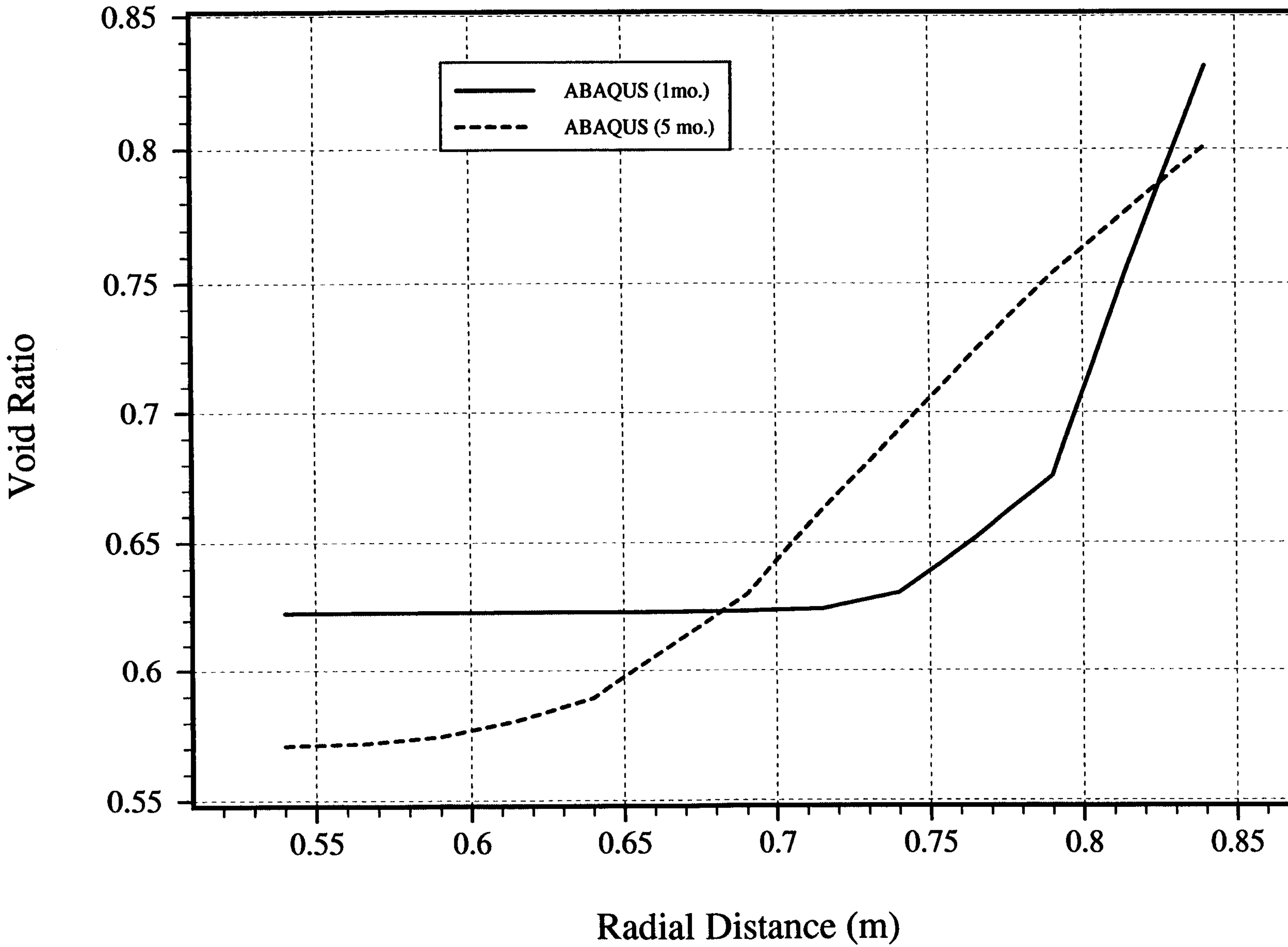

Figure 6-5. ABAQUS results for the void ratio through the buffer at a depth 3,000 mm below the ground surface (GL-3000), after elapsed times of 1 and 5 months

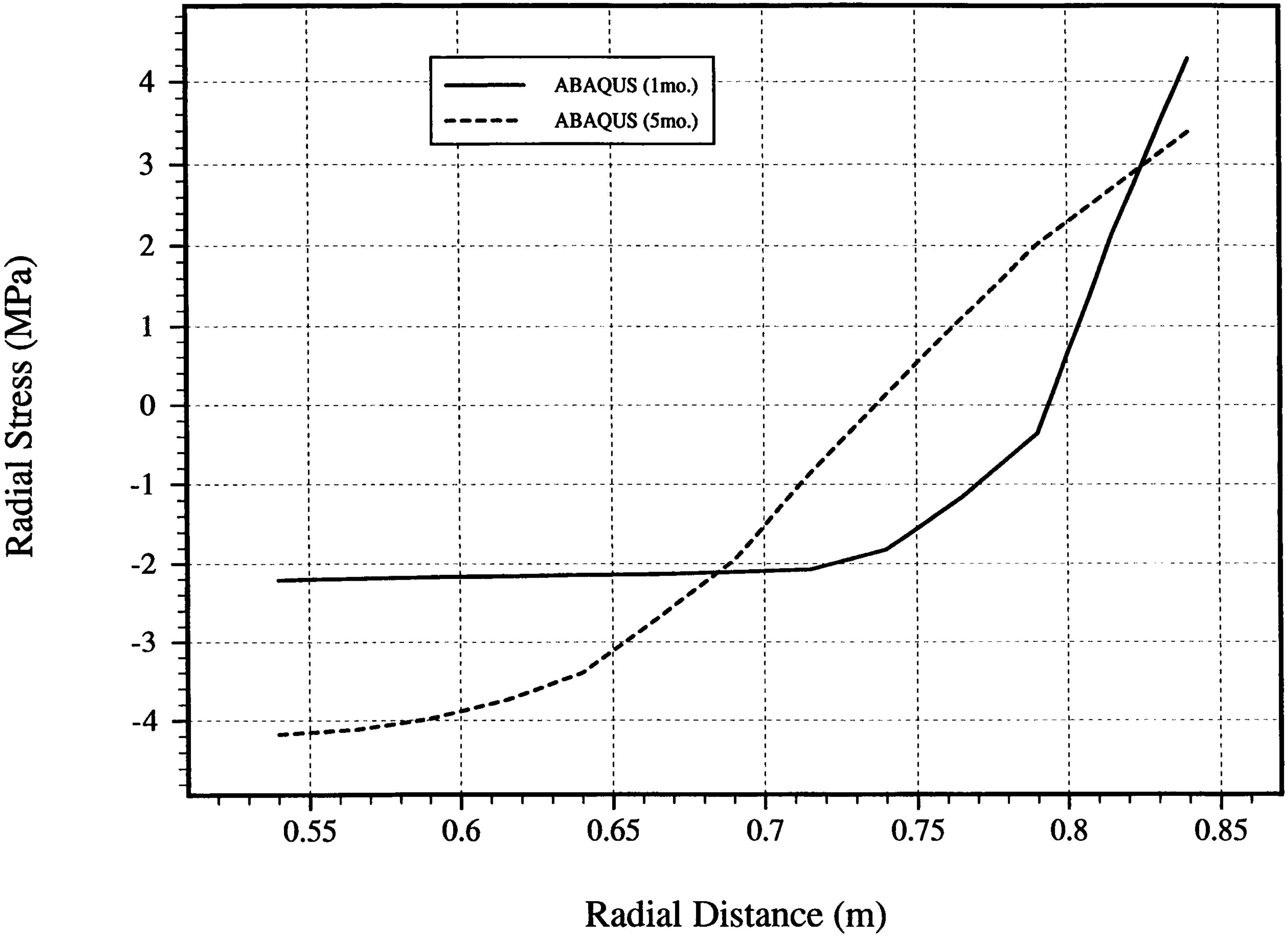

Figure 6-6. ABAQUS results for the radial stress through the buffer at a depth 3,000 mm below the ground surface (GL-3000), after elapsed times of 1 and 5 months (Compression negative)

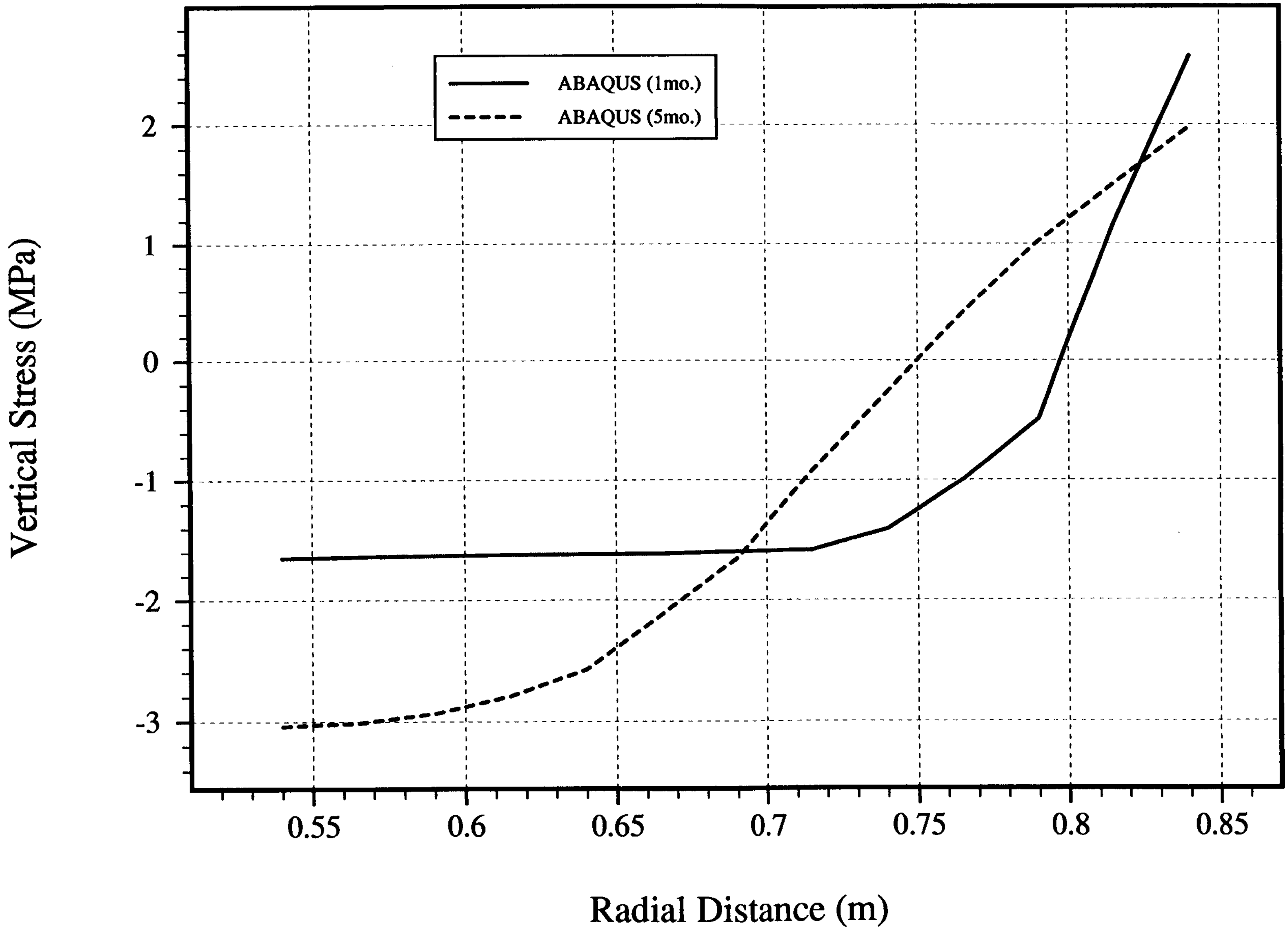

Figure 6-7. ABAQUS results for the vertical stress through the buffer at a depth 3,000 mm below the ground surface (GL-3000), after elapsed times of 1 and 5 months (Compression negative)

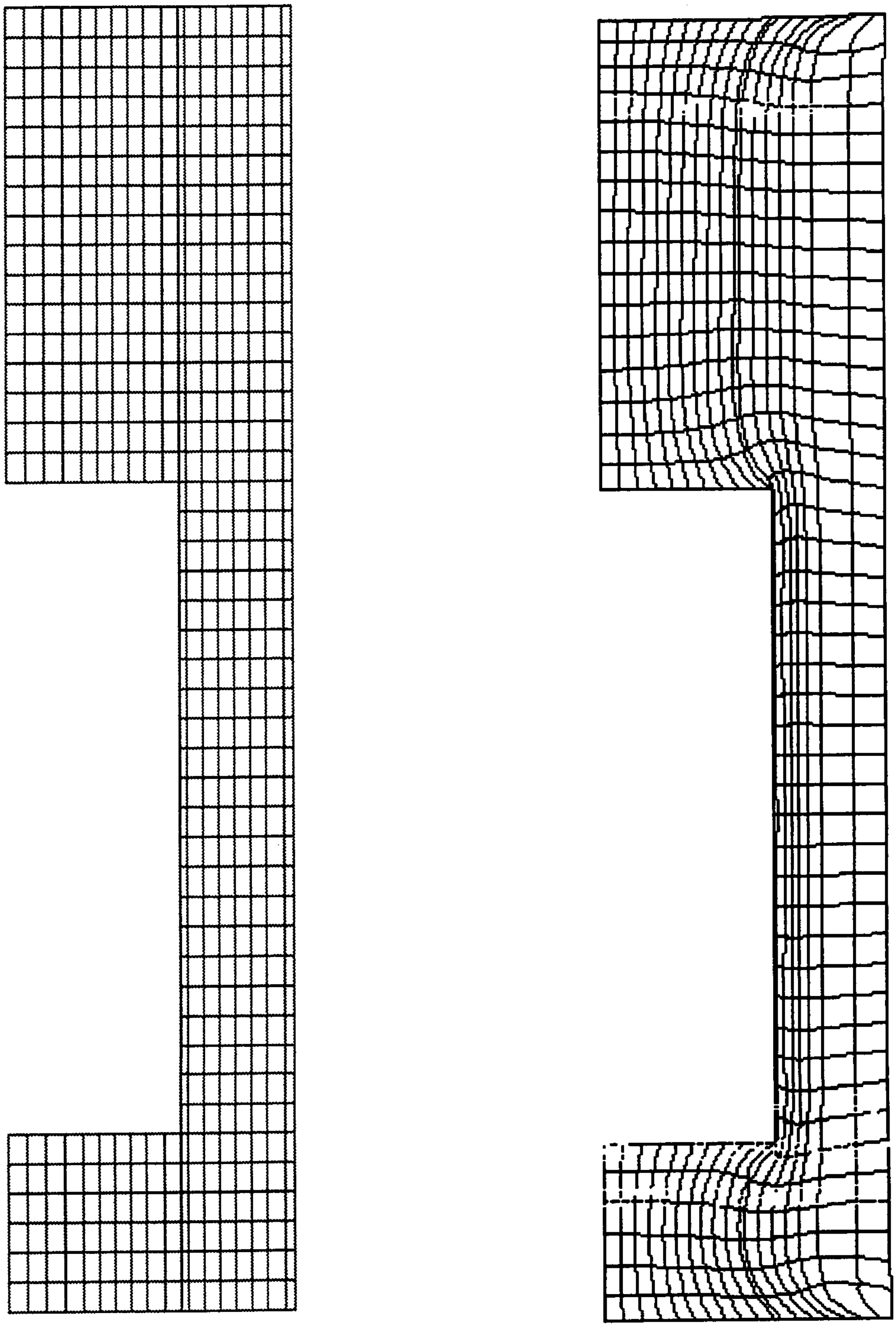

(a) (b)

Figure 6-8. ABAQUS mesh plot of the buffer region showing (a) initial undeformed mesh, and (b) deformed mesh after a time of 1 month (displacement magnification factor = 20)

7 DISCUSSION OF THE RESULTS

Interpretation of the results for this TC3 problem is difficult due to the number of coupled phenomena taking place simultaneously. Quite a number of variables are changing during the analysis making it difficult to isolate the reason for particular trends in the output, for example, the combination of both compression and tension within the bentonite. Also, in pure unsaturated flow analyses, the void ratio is usually assumed to remain constant, making it easy to visualize changes in saturation. However, in this particular problem, the void ratio is changing with the thermal expansion and swelling of the buffer material. Thus, the level of saturation could be changing as a result of both the influx of water as well as the change in void ratio of the solid material. The moisture retention curve specified for the buffer results in fairly large suction pressures in the partially saturated state. For instance at the initial saturation of 0.62, the initial suction pressure is approximately 15 MPa (Figure 4-3). Further investigation is necessary to determine if these suction pressures have a significant influence on the effective stress state or if the stress state is more dependent on the swelling and thermal expansion of the system. Likewise, the existence of high pore pressures and tensile stresses within the fully saturated concrete needs further investigation.

This TC3 problem is further complicated in that mechanical and hydrologic properties vary over many orders of magnitude. For example, the concrete is approximately three orders of magnitude stiffer than the bentonite. This in itself creates difficulties in obtaining stable solutions with the ABAQUS code. Trying to set the mechanical stiffness of the gap material lower than that of the bentonite as specified in Table 4-2 (i.e., original problem specifications) resulted in numerical instability unless the bentonite was allowed to swell significantly with increasing saturation. As a result, the thin gaps were assigned the same properties as the bentonite. It may be more appropriate to simulate the thin gaps using interface elements that would allow separation and likely eliminate the tensile stresses. Also, the bentonite may be better modeled as an inelastic material with swelling versus an elastic material with swelling. However, this was not explored.

Overall, the temperatures and water contents within the buffer material compare favorably. The stresses are highly dependent on the stiffness of the gap layers and the degree of swell versus saturation, both of which were not well known or adequately specified for this experiment. Consequently, it is not surprising that the calculated stresses do not agree with the experimental measurements.

8 RECOMMENDATIONS

Based on the modeling analysis of the Big-Ben Experiment (TC3) using ABAQUS, a number of recommendations can be made regarding future coupled THM analyses in a partially saturated medium. These recommendations hold particularly true for modeling predictions using ABAQUS of coupled THM processes at the potential Yucca Mountain repository site which also is in a partially saturated state. These recommendations are as follows:

- ABAQUS currently has no easy means of allowing material properties to vary with parameters other than temperature. In this particular TC3 problem, the mechanical and thermal properties of the buffer were experimentally determined to be strongly dependent on the water content. This has also been found to hold true based on preliminary study of the various rock units at the Yucca Mountain site. It would be beneficial to assess the amount of effort involved in upgrading the ABAQUS code to allow for this capability. It is likely that this could be accomplished through the development of a user defined subroutine to implement into the ABAQUS code.

- As mentioned in Section 6, ABAQUS only solves the flow equations for the wetting fluid. As a result, the code cannot simulate the drying effect, as is evident from the experimental measurements of water content in the buffer region adjacent to the heater. It is most likely that this drying effect is due to moisture being driven away in the vapor phase. It is desirable for ABAQUS to simulate both the liquid and vapor movement within a heated and partially saturated environment. Additional equations governing the gas flow would have to be incorporated into the code. If accurate predictions of the heat transfer and fluid flow are to be made for the Yucca Mountain repository site (specifically regarding the drying out of the near-field emplacement drifts and formation of condensation zones), it is believed that this capability is necessary especially if it is found that mechanical deformation of the rock matrix and fractures has an impact on this phenomenon. Otherwise, it may be sufficient to use any one of the available hydrologic codes capable of simulating the effect of evaporation/condensation. This capability has already been incorporated into one version of the ABAQUS code used by a one of the research teams involved in the DECOVALEX project (see Börgesson and Hernelind, 1994). It has not yet been established whether this particular version is available to the public.

9 SUMMARY AND CONCLUSIONS

A coupled TMH analysis of the Big-Ben Experiment (TC3) using ABAQUS as part of Phase III of the international cooperative project DECOVALEX is presented. Comparison has been made with some of the experimental measurement data provided in the specifications for this TC problem. The comparisons in general show good agreement among the temperatures except within the overpack very close to the heater. Slight discrepancies in the temperatures at other locations within the engineered barrier system can be attributed to the need for revised assumptions in the ABAQUS model regarding the thermal boundary conditions and thermal properties of the thin gap layers, both of which were poorly known or defined in the problem specifications. Comparison of the water contents in the bentonite at the end of the experiment show better agreement in the outer regions of the buffer material. The discrepancies in the inner region of the buffer adjacent to the heater can be attributed to the fact that ABAQUS cannot simulate the drying effect taking place in this region since it only tracks the behavior of the liquid or wetting fluid. It appears that in the actual experiment, moisture is being driven away in the vapor phase. Comparison of the stresses predicted by ABAQUS with those measured from pressure cells mounted to the wall of the borehole show little or no agreement. It is not conclusive at this time as to the reason for the disagreement. The experimental results appear to correctly measure an increasing swelling pressure with time along the borehole wall between the buffer and concrete. However, ABAQUS appears to incorrectly predict tension in this outer region of the bentonite as well as in the concrete itself. It is not clear if this is a result of the modeling approach taken or perhaps a result of the high suction in the inner portions of the buffer. It needs to be looked into more closely whether high suction pressures (as encountered in unsaturated conditions) can translate into fairly high mechanical pressures as seems to be the scheme adopted in ABAQUS. It is more commonly thought that hydrodynamic "suction" is a measure of how tightly the water is held in the unsaturated medium. Further comparisons/discussions of results obtained from the modeling teams with those measured experimentally will be given in the final DECOVALEX Phase III report to be published by the Swedish Nuclear Power Inspectorate in 1995.

10 REFERENCES

Ababou, R. 1991. *Approaches to Large Scale Unsaturated Flow in Heterogeneous, Stratified, and Fractured Geologic Media.* CNWRA 91-002. San Antonio, TX: Center for Nuclear Waste Regulatory Analyses.

Ababou, R., A. Millard, E. Treille, and M. Durin. 1993. *Coupled Thermo-Hydro-Mechanical Modeling for the Near Field Benchmark Test 3 (BMT3) of DECOVALEX Phase 2.* Draft Progress Report DMT/93/488. Paris, France:Commissariat A L'Energie Atomique.

Ahola, M.P., S.M. Hsiung, L.J. Lorig, and A.H. Chowdhury. 1992. *Thermo-Hydro-Mechanical Coupled Modeling: Multiple Fracture Model, BMT2; Coupled Stress-Flow Model, TC1. DECOVALEX - Phase I.* CNWRA 92-005. San Antonio, TX: Center for Nuclear Waste Regulatory Analyses.

Ahola, M.P., L.J. Lorig, A.H. Chowdhury, and S.M. Hsiung. 1993. *Thermo-Hydro-Mechanical Coupled Modeling: Near-Field Repository Model, BMT3. DECOVALEX - Phase II.* CNWRA 93-002. San Antonio, TX: Center for Nuclear Waste Regulatory Analyses.

Board, M. 1989a. *UDEC (Universal Distinct Element Code) Version 1.5.* Vols 1-3. NUREG/CR-5429. Washington, DC: Nuclear Regulatory Commission.

Board, M. 1989b. *FLAC (Fast Lagrangian Analysis of Continua) Version 2.20.*Vols 1-3. NUREG/CR-5430. Washington, DC: Nuclear Regulatory Commission.

Börgesson, L., and J. Hernelind. 1994. *Calculation of Test Case 3 — Big Ben Experiment.* DECOVALEX Phase III. Draft Report. Lund, Sweden: Clay Technology AB.

DECOVALEX. 1993a. *Test Case 6, Borehole Injection Test,* DECOVALEX Doc 93/139. DECOVALEX Secretariat. Stockholm, Sweden: Royal Institute of Technology.

DECOVALEX. 1993b. Phase 3, *Test Case 3, Big Ben,* DECOVALEX Doc 93/124. DECOVALEX Secretariat. Stockholm, Sweden: Royal Institute of Technology

Fujita, T., K. Hara, Y. Yusa, and N. Sasaki. 1991. *Application of Elasto-Plastic Model to Mechanical and Hydraulic Behavior of Buffer Material under Water Uptake in a Repository.* Materials Research Society Symposium. Vol. 212. Materials Research Society.

Ghosh, A., S.M. Hsiung, G.I. Ofoegbu, and A.H. Chowdhury. 1994. *Evaluation of Computer Codes for Compliance Determination Phase II.* CNWRA 94-001. San Antonio, TX: Center for Nuclear Waste Regulatory Analyses.

Green, R.T., R.D. Manteufel, F.T. Dodge, and S.J. Svedeman. 1993. *Theoretical and Experimental Investigation of Thermohydrologic Processes in a Partially Saturated, Fractured Porous Medium.* NUREG/CR-6026. Washington, DC: Nuclear Regulatory Commission.

Gros, J.C. 1992. Fanay-Augeres THM Test. *DECOVALEX Phase 3 Test-Case.* IPSN Report 92/43. Paris, France: Institut De Protection Et De Surete. Nucleaire.

Hibbitt, Karlsson & Sorensen, Inc. 1992. *ABAQUS/Standard User's Manual.* Version 5.3. Pawtucket, RI: Hibbitt, Karlsson & Sorenson, Inc.

Jing, L., J. Rutqvist, O. Stephansson, C.F. Tsang, and F. Kautsky. 1993. *DECOVALEX - Mathematical Models of Coupled T-H-M Processes for Nuclear Waste Repositories - Report of Phase I.* SKI Technical Report 93-31. Stockholm, Sweden: Swedish Nuclear Power Inspectorate.

Jing, L., J. Rutqvist, O. Stephansson, C.F. Tsang, and F. Kautsky. 1994. *DECOVALEX - Mathematical Models of Coupled T-H-M Processes for Nuclear Waste Repositories - Report of Phase II.* Stockholm, Sweden: Swedish Nuclear Power Inspectorate.

Kana, D.D., B.H.G. Brady, B.W. Vanzant, and P.K. Nair. 1991. *Critical Assessment of Seismic and Geomechanics Literature Related to a High-Level Nuclear Waste Underground Repository.* NUREG/CR-5440. Washington, DC: Nuclear Regulatory Commission.

Laboratory of Rock Engineering. 1993. *Determination of the Coupled Behavior of a Rock Joint by Using Digitally Controlled Rock Mechanics Testing System.* Ver. 2.0. Espoo, Finland: Helsinki University of Technology.

Manteufel, R.D., M.P. Ahola, D.R. Turner, and A.H. Chowdhury. 1993. *A Literature Review of Coupled Thermal-Hydrologic-Mechanical-Chemical Processes Pertinent to the Proposed High-Level Nuclear Waste Repository.* NUREG/CR-6021. Washington, DC: Nuclear Regulatory Commission.

Mitchell, J.K. 1976. *Fundamentals of Soil Behavior.* New York, NY: John Wiley & Sons, Inc.

Mohanty, S. 1994. *Experimental Investigation of Hydraulic Conductivity of Apache Leap Tuff Under Normal and Shear Loads.* San Antonio, TX: Center for Nuclear Waste Regulatory Analyses (In Process).

Noorishad, J., and C.F. Tsang. 1989. *Recent Enhancement of the Coupled Hydro-Mechanical Code: ROCMAS II.* Technical Report 89:4. Stockholm, Sweden: Swedish Nuclear Power Inspectorate.

Ohnishi, Y., H. Shibata, and A. Kobayashi. 1985. Development of finite element code for the analysis of coupled thermo-hydro-mechanical behavior of saturated-unsaturated medium. *Proceedings of the International Symposium on Coupled Processes Affecting the Performance of a Nuclear Waste Repository.* Berkeley, CA: 263–268.

Tijani, S.M. 1991. *VIPLEF, CHEF, HYDREF - User's Guide.* Paris, France: Paris School of Mines (ENSMP).

Tsang, C.F. 1991. Coupled thermomechanical hydrochemical processes in rock fractures. *Review of Geophysics* 29: 537–551.

APPENDIX A

ABAQUS INPUT FILE FOR THE TC3 PROBLEM (THERMAL ANALYSIS)

```
*HEADING
ABAQUS Heat Transfer Model of BIG-BEN Experiment
*PREPRINT,ECHO=NO,MODEL=NO,HISTORY=NO
*RESTART,WRITE,FREQUENCY=1,OVERLAY
***
*** Nodal data
*** 8-node element case
*** Convection boundary conditions applied.
***
*NODE
101,0.0,0.0
109,0.22,0.0
121,0.52,0.0
123,0.54,0.0
135,0.84,0.0
137,0.87,0.0
155,3.0,0.0
**
1101,0.0,0.45
1109,0.22,0.45
1121,0.52,0.45
1123,0.54,0.45
1135,0.84,0.45
1137,0.87,0.45
1155,3.0,0.45
**
2301,0.0,0.95
2309,0.22,0.95
2321,0.52,0.95
2323,0.54,0.95
2335,0.84,0.95
2337,0.87,0.95
2355,3.0,0.95
**
3501,0.0,1.45
3509,0.22,1.45
3521,0.52,1.45
3523,0.54,1.45
3535,0.84,1.45
3537,0.87,1.45
3555,3.0,1.45
**
5501,0.0,2.45
5509,0.22,2.45
5521,0.52,2.45
5523,0.54,2.45
5535,0.84,2.45
5537,0.87,2.45
5555,3.0,2.45
**
6701,0.0,2.9
6709,0.22,2.9
6721,0.52,2.9
6723,0.54,2.9
6735,0.84,2.9
6737,0.87,2.9
6755,3.0,2.9
**
9901,0.0,4.4
9909,0.22,4.4
```

```
9921,0.52,4.4
9923,0.54,4.4
9935,0.84,4.4
9937,0.87,4.4
9955,3.0,4.4
**
11101,0.0,5.0
11109,0.22,5.0
11121,0.52,5.0
11123,0.54,5.0
11135,0.84,5.0
11137,0.87,5.0
11155,3.0,5.0
**
*NGEN, NSET=VL1
101,11101,100
*NGEN, NSET=VL2
109,11109,100
*NFILL,NSET=NTOT
VL1,VL2,8,1
*NCOPY, CHANGE NUMBER=12, OLD SET=VL2, SHIFT, NEW SET=VL3
0.30,0.0,0.0
0.0,0.0,0.0,0.0,0.0,1.0,0.0
*NFILL,NSET=NTOT
VL2,VL3,12,1
*NCOPY, CHANGE NUMBER=2, OLD SET=VL3, SHIFT, NEW SET=VL4
0.02,0.0,0.0
0.0,0.0,0.0,0.0,0.0,1.0,0.0
*NFILL,NSET=NTOT
VL3,VL4,2,1
*NCOPY, CHANGE NUMBER=12, OLD SET=VL4, SHIFT, NEW SET=VL5
0.30,0.0,0.0
0.0,0.0,0.0,0.0,0.0,1.0,0.0
*NFILL,NSET=NTOT
VL4,VL5,12,1
*NCOPY, CHANGE NUMBER=2, OLD SET=VL5, SHIFT, NEW SET=VL6
0.03,0.0,0.0
0.0,0.0,0.0,0.0,0.0,1.0,0.0
*NFILL,NSET=NTOT
VL5,VL6,2,1
*NCOPY, CHANGE NUMBER=18, OLD SET=VL6, SHIFT, NEW SET=VL7
2.13,0.0,0.0
0.0,0.0,0.0,0.0,0.0,1.0,0.0
*NFILL, BIAS=0.8,TWOSTEP,NSET=NTOT
VL6,VL7,18,1
*NSET, NSET=LEFT, GENERATE
101,11101,100
*NSET, NSET=RIGHT, GENERATE
155,11155,100
*NSET, NSET=TOP, GENERATE
11101,11155,1
*NSET, NSET=BOTTOM, GENERATE
101,155,1
**
** ELEMENT DEFINITIONS
**
*ELEMENT, TYPE=DCAX8
101,101,103,303,301,102,203,302,201
*ELGEN
101,27,2,1,55,200,100
```

```
*ELSET, ELSET=GLASS, GENERATE
1801,2701,100
1802,2702,100
1803,2703,100
1804,2704,100
*ELSET, ELSET=OVPACK, GENERATE
1201,1701,100
1202,1702,100
1203,1703,100
1204,1704,100
2801,3301,100
2802,3302,100
2803,3303,100
2804,3304,100
1205,3305,100
1206,3306,100
1207,3307,100
1208,3308,100
1209,3309,100
1210,3310,100
*ELSET, ELSET=GAP, GENERATE
1211,3311,100
618,4918,100
*ELSET, ELSET=BENT, GENERATE
601,1101,100
602,1102,100
603,1103,100
604,1104,100
605,1105,100
606,1106,100
607,1107,100
608,1108,100
609,1109,100
610,1110,100
611,1111,100
3401,4901,100
3402,4902,100
3403,4903,100
3404,4904,100
3405,4905,100
3406,4906,100
3407,4907,100
3408,4908,100
3409,4909,100
3410,4910,100
3411,4911,100
612,4912,100
613,4913,100
614,4914,100
615,4915,100
616,4916,100
617,4917,100
*ELSET, ELSET=CONCRETE, GENERATE
101,501,100
102,502,100
103,503,100
104,504,100
105,505,100
106,506,100
107,507,100
```

```
108,508,100
109,509,100
110,510,100
111,511,100
112,512,100
113,513,100
114,514,100
115,515,100
116,516,100
117,517,100
118,518,100
5001,5501,100
5002,5502,100
5003,5503,100
5004,5504,100
5005,5505,100
5006,5506,100
5007,5507,100
5008,5508,100
5009,5509,100
5010,5510,100
5011,5511,100
5012,5512,100
5013,5513,100
5014,5514,100
5015,5515,100
5016,5516,100
5017,5517,100
5018,5518,100
119,5519,100
120,5520,100
121,5521,100
122,5522,100
123,5523,100
124,5524,100
125,5525,100
126,5526,100
127,5527,100
*ELSET, ELSET=LEFT1, GENERATE
101,5501,100
*ELSET, ELSET=TOP1, GENERATE
5501,5528,1
*ELSET, ELSET=RIGHT1, GENERATE
127,5527,100
*ELSET, ELSET=BOTTOM1, GENERATE
101,127,1
*ELSET, ELSET=HEATER, GENERATE
1801,2701,100
**
**ELEMENT PROPERTIES
**
*SOLID SECTION,ELSET=GLASS,MATERIAL=MAT1
*MATERIAL,NAME=MAT1
*CONDUCTIVITY
0.255
*DENSITY
1600.0
*SPECIFIC HEAT
840.0
*SOLID SECTION,ELSET=OVPACK,MATERIAL=MAT2
```

```
*MATERIAL,NAME=MAT2
*CONDUCTIVITY
53.0
*DENSITY
7800.0
*SPECIFIC HEAT
460.0
***
*** GAP zone now assigned the same thermal properties as for BENT zone(GIO)
***
*SOLID SECTION,ELSET=GAP,MATERIAL=MAT4
***
*SOLID SECTION,ELSET=BENT,MATERIAL=MAT4
*MATERIAL,NAME=MAT4
*CONDUCTIVITY
1.148
*DENSITY
1860.0
*SPECIFIC HEAT
1453.0
*SOLID SECTION,ELSET=CONCRETE,MATERIAL=MAT5
*MATERIAL,NAME=MAT5
*CONDUCTIVITY
1.88
*DENSITY
2300.0
*SPECIFIC HEAT
750.0
**
*INITIAL CONDITIONS, TYPE=TEMPERATURE
NTOT, 15.0
*AMPLITUDE, NAME=H3
0.0,1.0,1.0E15,1.0
***
*** Run Transient Analysis
***
*** Step 1: To end of first hour
***
*STEP, INC=2000
*HEAT TRANSFER,DELTMX=5.0
1.0,3.6E3
***
*** Convective B.C.
***
*FILM, AMPLITUDE=H3
TOP1,F3,15.0,0.5
RIGHT1,F2,15.0,0.5
BOTTOM1,F1,15.0,0.5
***
***  Volumetric heat flux (W/m**3)
***
*DFLUX, AMPLITUDE=H3
HEATER,BF,8.4184E4
*RESTART, WRITE, FREQUENCY=5000
*NODE PRINT,FREQUENCY=0
*EL PRINT,FREQUENCY=0
*NODE FILE, NSET=NTOT, FREQUENCY=50000
NT
*END STEP
***
```

```
*** Step 2: To end of first day
***
*STEP, INC=2000
*HEAT TRANSFER,DELTMX=5.0
1.8E2,8.28E4
*RESTART, WRITE, FREQUENCY=5000
*NODE PRINT,FREQUENCY=0
*EL PRINT,FREQUENCY=0
*NODE FILE, NSET=NTOT, FREQUENCY=50000
NT
*END STEP
***
*** Step 3: To end of first 10 days
***
*STEP, INC=2000
*HEAT TRANSFER,DELTMX=5.0
3.6E3,7.776E5
*RESTART, WRITE, FREQUENCY=5000
*NODE PRINT,FREQUENCY=0
*EL PRINT,FREQUENCY=0
*NODE FILE, NSET=NTOT, FREQUENCY=50000
NT
*END STEP
***
*** Step 4: To end of first 20 days
***
*STEP, INC=2000
*HEAT TRANSFER,DELTMX=5.0
3.6E3,8.64E5
*RESTART, WRITE, FREQUENCY=5000
*NODE PRINT,FREQUENCY=0
*EL PRINT,FREQUENCY=0
*NODE FILE, NSET=NTOT, FREQUENCY=50000
NT
*END STEP
***
*** Step 5: To end of first month
***
*STEP, INC=2000
*HEAT TRANSFER,DELTMX=5.0
3.6E3,8.64E5
*RESTART, WRITE, FREQUENCY=5000
*NODE PRINT,FREQUENCY=0
*EL PRINT,FREQUENCY=0
*NODE FILE, NSET=NTOT, FREQUENCY=50000
NT
*END STEP
***
*** Step 6: To end of 1 month, 10 days
***
*STEP, INC=2000
*HEAT TRANSFER,DELTMX=5.0
3.6E3,8.64E5
*RESTART, WRITE, FREQUENCY=5000
*NODE PRINT,FREQUENCY=0
*EL PRINT,FREQUENCY=0
*NODE FILE, NSET=NTOT, FREQUENCY=50000
NT
*END STEP
***
```

```
*** Step 7: To end of 1 month, 20 days
***
*STEP, INC=2000
*HEAT TRANSFER,DELTMX=5.0
3.6E3,8.64E5
*RESTART, WRITE, FREQUENCY=5000
*NODE PRINT,FREQUENCY=0
*EL PRINT,FREQUENCY=0
*NODE FILE, NSET=NTOT, FREQUENCY=50000
NT
*END STEP
***
*** Step 8: To end of second month
***
*STEP, INC=2000
*HEAT TRANSFER,DELTMX=5.0
3.6E3,8.64E5
*RESTART, WRITE, FREQUENCY=5000
*NODE PRINT,FREQUENCY=0
*EL PRINT,FREQUENCY=0
*NODE FILE, NSET=NTOT, FREQUENCY=50000
NT
*END STEP
***
*** Step 9: To end of 2 months, 10 days
***
*STEP, INC=2000
*HEAT TRANSFER,DELTMX=5.0
3.6E3,8.64E5
*RESTART, WRITE, FREQUENCY=5000
*NODE PRINT,FREQUENCY=0
*EL PRINT,FREQUENCY=0
*NODE FILE, NSET=NTOT, FREQUENCY=50000
NT
*END STEP
***
*** Step 10: To end of 2 months, 20 days
***
*STEP, INC=2000
*HEAT TRANSFER,DELTMX=5.0
3.6E3,8.64E5
*RESTART, WRITE, FREQUENCY=5000
*NODE PRINT,FREQUENCY=0
*EL PRINT,FREQUENCY=0
*NODE FILE, NSET=NTOT, FREQUENCY=50000
NT
*END STEP
***
*** Step 11: To end of 3 months
***
*STEP, INC=2000
*HEAT TRANSFER,DELTMX=5.0
3.6E3,8.64E5
*RESTART, WRITE, FREQUENCY=5000
*NODE PRINT,FREQUENCY=0
*EL PRINT,FREQUENCY=0
*NODE FILE, NSET=NTOT, FREQUENCY=50000
NT
*END STEP
***
```

```
*** Step 12: To end of 3 months, 10 days
***
*STEP, INC=2000
*HEAT TRANSFER,DELTMX=5.0
3.6E3,8.64E5
*RESTART, WRITE, FREQUENCY=5000
*NODE PRINT,FREQUENCY=0
*EL PRINT,FREQUENCY=0
*NODE FILE, NSET=NTOT, FREQUENCY=50000
NT
*END STEP
***
*** Step 13: To end of 3 months, 20 days
***
*STEP, INC=2000
*HEAT TRANSFER,DELTMX=5.0
3.6E3,8.64E5
*RESTART, WRITE, FREQUENCY=5000
*NODE PRINT,FREQUENCY=0
*EL PRINT,FREQUENCY=0
*NODE FILE, NSET=NTOT, FREQUENCY=50000
NT
*END STEP
***
*** Step 14: To end of 4 months
***
*STEP, INC=2000
*HEAT TRANSFER,DELTMX=5.0
3.6E3,8.64E5
*RESTART, WRITE, FREQUENCY=5000
*NODE PRINT,FREQUENCY=0
*EL PRINT,FREQUENCY=0
*NODE FILE, NSET=NTOT, FREQUENCY=50000
NT
*END STEP
***
*** Step 15: To end of 4 months, 10 days
***
*STEP, INC=2000
*HEAT TRANSFER,DELTMX=5.0
3.6E3,8.64E5
*RESTART, WRITE, FREQUENCY=5000
*NODE PRINT,FREQUENCY=0
*EL PRINT,FREQUENCY=0
*NODE FILE, NSET=NTOT, FREQUENCY=50000
NT
*END STEP
***
*** Step 16: To end of 4 months, 20 days
***
*STEP, INC=2000
*HEAT TRANSFER,DELTMX=5.0
3.6E3,8.64E5
*RESTART, WRITE, FREQUENCY=5000
*NODE PRINT,FREQUENCY=0
*EL PRINT,FREQUENCY=0
*NODE FILE, NSET=NTOT, FREQUENCY=50000
NT
*END STEP
***
```

```
*** Step 17: To end of 5 months
***
*STEP, INC=2000
*HEAT TRANSFER,DELTMX=5.0
3.6E3,8.64E5
*RESTART, WRITE, FREQUENCY=5000
*NODE PRINT,FREQUENCY=0
*EL PRINT,FREQUENCY=0
*NODE FILE, NSET=NTOT, FREQUENCY=50000
NT
*END STEP
```

APPENDIX B

ABAQUS INPUT FILE FOR THE TC3 PROBLEM (POROELASTIC ANALYSIS)

```
*HEADING
ABAQUS coupled Stress/Porous Flow Model of BIG-BEN Experiment
**** Gap properties assigned same mechanical stiffness as the benonite.
**** Moisture swelling allowed in bentonite.
*PREPRINT,ECHO=NO,MODEL=NO,HISTORY=NO
*RESTART,WRITE,FREQUENCY=1,OVERLAY
***
*** Nodal data
*** 8-node element case
***
*NODE
101,0.0,0.0
109,0.22,0.0
121,0.52,0.0
123,0.54,0.0
135,0.84,0.0
137,0.87,0.0
155,3.0,0.0
**
1101,0.0,0.45
1109,0.22,0.45
1121,0.52,0.45
1123,0.54,0.45
1135,0.84,0.45
1137,0.87,0.45
1155,3.0,0.45
**
2301,0.0,0.95
2309,0.22,0.95
2321,0.52,0.95
2323,0.54,0.95
2335,0.84,0.95
2337,0.87,0.95
2355,3.0,0.95
**
3501,0.0,1.45
3509,0.22,1.45
3521,0.52,1.45
3523,0.54,1.45
3535,0.84,1.45
3537,0.87,1.45
3555,3.0,1.45
**
5501,0.0,2.45
5509,0.22,2.45
5521,0.52,2.45
5523,0.54,2.45
5535,0.84,2.45
5537,0.87,2.45
5555,3.0,2.45
**
6701,0.0,2.9
6709,0.22,2.9
6721,0.52,2.9
6723,0.54,2.9
6735,0.84,2.9
6737,0.87,2.9
6755,3.0,2.9
**
9901,0.0,4.4
```

```
9909,0.22,4.4
9921,0.52,4.4
9923,0.54,4.4
9935,0.84,4.4
9937,0.87,4.4
9955,3.0,4.4
**
11101,0.0,5.0
11109,0.22,5.0
11121,0.52,5.0
11123,0.54,5.0
11135,0.84,5.0
11137,0.87,5.0
11155,3.0,5.0
**
*NGEN, NSET=VL1
101,11101,100
*NGEN, NSET=VL2
109,11109,100
*NFILL,NSET=NTOT
VL1,VL2,8,1
*NCOPY, CHANGE NUMBER=12, OLD SET=VL2, SHIFT, NEW SET=VL3
0.30,0.0,0.0
0.0,0.0,0.0,0.0,0.0,1.0,0.0
*NFILL,NSET=NTOT
VL2,VL3,12,1
*NCOPY, CHANGE NUMBER=2, OLD SET=VL3, SHIFT, NEW SET=VL4
0.02,0.0,0.0
0.0,0.0,0.0,0.0,0.0,1.0,0.0
*NFILL,NSET=NTOT
VL3,VL4,2,1
*NCOPY, CHANGE NUMBER=12, OLD SET=VL4, SHIFT, NEW SET=VL5
0.30,0.0,0.0
0.0,0.0,0.0,0.0,0.0,1.0,0.0
*NFILL,NSET=NTOT
VL4,VL5,12,1
*NCOPY, CHANGE NUMBER=2, OLD SET=VL5, SHIFT, NEW SET=VL6
0.03,0.0,0.0
0.0,0.0,0.0,0.0,0.0,1.0,0.0
*NFILL,NSET=NTOT
VL5,VL6,2,1
*NCOPY, CHANGE NUMBER=18, OLD SET=VL6, SHIFT, NEW SET=VL7
2.13,0.0,0.0
0.0,0.0,0.0,0.0,0.0,1.0,0.0
*NFILL, BIAS=0.8,TWOSTEP,NSET=NTOT
VL6,VL7,18,1
*NSET, NSET=LEFT, GENERATE
101,11101,100
*NSET, NSET=RIGHT_FL, GENERATE
355,10955,200
*NSET, NSET=TOP_FL, GENERATE
11101,11155,2
*NSET, NSET=BOT_FL, GENERATE
101,155,2
*NSET, NSET=BOT_DIS, GENERATE
101,155,1
*NSET, NSET=CRACK, GENERATE
1137,9937,200
*NSET, NSET=NBENT, GENERATE
1101,2301,200
```

```
1103,2303,200
1105,2305,200
1107,2307,200
1109,2309,200
1111,2311,200
1113,2313,200
1115,2315,200
1117,2317,200
1119,2319,200
6701,9901,200
6703,9903,200
6705,9905,200
6707,9907,200
6709,9909,200
6711,9911,200
6713,9913,200
6715,9915,200
6717,9917,200
6719,9919,200
1121,9921,200
1123,9923,200
1125,9925,200
1127,9927,200
1129,9929,200
1131,9931,200
1133,9933,200
1135,9935,200
1137,9937,200
*NSET, NSET=NCONC, GENERATE
101,901,200
103,903,200
105,905,200
107,907,200
109,909,200
111,911,200
113,913,200
115,915,200
117,917,200
119,919,200
121,921,200
123,923,200
125,925,200
127,927,200
129,929,200
131,931,200
133,933,200
135,935,200
137,937,200
10101,11101,200
10103,11103,200
10105,11105,200
10107,11107,200
10109,11109,200
10111,11111,200
10113,11113,200
10115,11115,200
10117,11117,200
10119,11119,200
10121,11121,200
10123,11123,200
```

```
10125,11125,200
10127,11127,200
10129,11129,200
10131,11131,200
10133,11133,200
10135,11135,200
10137,11137,200
139,11139,200
141,11141,200
143,11143,200
145,11145,200
147,11147,200
149,11149,200
151,11151,200
153,11153,200
155,11155,200
**
** ELEMENT DEFINITIONS
**
*ELEMENT, TYPE=CAX8R
1201,2301,2303,2503,2501,2302,2403,2502,2401
*ELGEN
1201,10,2,1,22,200,100
*ELEMENT,TYPE=CAX8RP
601,1101,1103,1303,1301,1102,1203,1302,1201
*ELGEN
601,18,2,1,6,200,100
*ELEMENT,TYPE=CAX8RP
1211,2321,2323,2523,2521,2322,2423,2522,2421
*ELGEN
1211,8,2,1,22,200,100
*ELEMENT,TYPE=CAX8RP
3401,6701,6703,6903,6901,6702,6803,6902,6801
*ELGEN
3401,18,2,1,16,200,100
*ELEMENT, TYPE=CAX8RP
101,101,103,303,301,102,203,302,201
*ELGEN
101,18,2,1,5,200,100
*ELEMENT, TYPE=CAX8RP
119,137,139,339,337,138,239,338,237
*ELGEN
119,9,2,1,55,200,100
*ELEMENT, TYPE=CAX8RP
5001,9901,9903,10103,10101,9902,10003,10102,10001
*ELGEN
5001,18,2,1,6,200,100
******
******
*ELSET, ELSET=GLASS, GENERATE
1801,2701,100
1802,2702,100
1803,2703,100
1804,2704,100
*ELSET, ELSET=OVPACK, GENERATE
1201,1701,100
1202,1702,100
1203,1703,100
1204,1704,100
2801,3301,100
```

```
2802,3302,100
2803,3303,100
2804,3304,100
1205,3305,100
1206,3306,100
1207,3307,100
1208,3308,100
1209,3309,100
1210,3310,100
*ELSET, ELSET=BENT, GENERATE
601,1101,100
602,1102,100
603,1103,100
604,1104,100
605,1105,100
606,1106,100
607,1107,100
608,1108,100
609,1109,100
610,1110,100
3401,4901,100
3402,4902,100
3403,4903,100
3404,4904,100
3405,4905,100
3406,4906,100
3407,4907,100
3408,4908,100
3409,4909,100
3410,4910,100
611,4911,100
612,4912,100
613,4913,100
614,4914,100
615,4915,100
616,4916,100
617,4917,100
618,4918,100
*ELSET, ELSET=CONCRETE, GENERATE
101,501,100
102,502,100
103,503,100
104,504,100
105,505,100
106,506,100
107,507,100
108,508,100
109,509,100
110,510,100
111,511,100
112,512,100
113,513,100
114,514,100
115,515,100
116,516,100
117,517,100
118,518,100
5001,5501,100
5002,5502,100
5003,5503,100
```

```
5004,5504,100
5005,5505,100
5006,5506,100
5007,5507,100
5008,5508,100
5009,5509,100
5010,5510,100
5011,5511,100
5012,5512,100
5013,5513,100
5014,5514,100
5015,5515,100
5016,5516,100
5017,5517,100
5018,5518,100
119,5519,100
120,5520,100
121,5521,100
122,5522,100
123,5523,100
124,5524,100
125,5525,100
126,5526,100
127,5527,100
*ELSET, ELSET=LEFT1, GENERATE
101,5501,100
*ELSET, ELSET=TOP1, GENERATE
5501,5527,1
*ELSET, ELSET=RIGHT1, GENERATE
127,5527,100
*ELSET, ELSET=BOTTOM1, GENERATE
101,127,1
*ELSET, ELSET=HEATER, GENERATE
1801,2701,100
*ELSET, ELSET=ELOUTPT, GENERATE
1112,1117,1
1212,1217,1
2212,2217,1
2312,2317,1
3901,3917,1
4001,4017,1
*ELSET, ELSET=ELTOT
GLASS,OVPACK,BENT,CONCRETE
**
**ELEMENT PROPERTIES
**
*SOLID SECTION,ELSET=GLASS,MATERIAL=MAT1
*MATERIAL,NAME=MAT1
*ELASTIC
8.20E4,0.30
*DENSITY
1600.0E-6
*EXPANSION
1.0E-05
*SOLID SECTION,ELSET=OVPACK,MATERIAL=MAT2
*MATERIAL,NAME=MAT2
*ELASTIC
2.0E5,0.30
*DENSITY
7800.0E-6
```

```
*EXPANSION
1.64E-06
*SOLID SECTION,ELSET=BENT,MATERIAL=MAT3
*MATERIAL,NAME=MAT3
*ELASTIC
27.0,0.4
*POROUS BULK MODULI
5.0E4,2.0E3
*DENSITY
1860.0E-6
*EXPANSION
1.0E-04
*EXPANSION, PORE FLUID
1.667E-4
**
*SORPTION
-.1392E+04,    0.0261
-.7319E+03,    0.0323
-.3848E+03,    0.0445
-.2021E+03,    0.0690
-.1385E+03,    0.0935
-.1058E+03,    0.1180
-.8579E+02,    0.1425
-.7218E+02,    0.1670
-.6229E+02,    0.1915
-.5475E+02,    0.2160
-.4880E+02,    0.2405
-.4397E+02,    0.2650
-.3996E+02,    0.2895
-.3657E+02,    0.3140
-.3366E+02,    0.3385
-.3112E+02,    0.3630
-.2889E+02,    0.3875
-.2690E+02,    0.4120
-.2511E+02,    0.4365
-.2350E+02,    0.4610
-.2202E+02,    0.4855
-.2067E+02,    0.5100
-.1942E+02,    0.5345
-.1825E+02,    0.5590
-.1716E+02,    0.5835
-.1614E+02,    0.6080
-.1517E+02,    0.6325
-.1425E+02,    0.6570
-.1337E+02,    0.6815
-.1252E+02,    0.7060
-.1170E+02,    0.7305
-.1090E+02,    0.7550
-.1011E+02,    0.7795
-.9336E+01,    0.8040
-.8561E+01,    0.8285
-.7780E+01,    0.8530
-.6979E+01,    0.8775
-.6143E+01,    0.9020
-.5246E+01,    0.9265
-.4235E+01,    0.9510
-.2979E+01,    0.9755
-.2115E+01,    0.9877
 .0       ,    1.0000
*SORPTION,TYPE=EXSORPTION
```

```
-.1392E+04,     0.0261
-.7319E+03,     0.0323
-.3848E+03,     0.0445
-.2021E+03,     0.0690
-.1385E+03,     0.0935
-.1058E+03,     0.1180
-.8579E+02,     0.1425
-.7218E+02,     0.1670
-.6229E+02,     0.1915
-.5475E+02,     0.2160
-.4880E+02,     0.2405
-.4397E+02,     0.2650
-.3996E+02,     0.2895
-.3657E+02,     0.3140
-.3366E+02,     0.3385
-.3112E+02,     0.3630
-.2889E+02,     0.3875
-.2690E+02,     0.4120
-.2511E+02,     0.4365
-.2350E+02,     0.4610
-.2202E+02,     0.4855
-.2067E+02,     0.5100
-.1942E+02,     0.5345
-.1825E+02,     0.5590
-.1716E+02,     0.5835
-.1614E+02,     0.6080
-.1517E+02,     0.6325
-.1425E+02,     0.6570
-.1337E+02,     0.6815
-.1252E+02,     0.7060
-.1170E+02,     0.7305
-.1090E+02,     0.7550
-.1011E+02,     0.7795
-.9336E+01,     0.8040
-.8561E+01,     0.8285
-.7780E+01,     0.8530
-.6979E+01,     0.8775
-.6143E+01,     0.9020
-.5246E+01,     0.9265
-.4235E+01,     0.9510
-.2979E+01,     0.9755
-.2115E+01,     0.9877
 .0        ,    1.0000
*PERMEABILITY, SPECIFIC=0.01
4.0E-13,0.695
*PERMEABILITY,SPECIFIC=0.01,TYPE=SATURATION
0.6800E-10,     0.0261
0.1391E-08,     0.0323
0.2846E-07,     0.0445
0.5829E-06,     0.0690
0.3413E-05,     0.0935
0.1197E-04,     0.1180
0.3174E-04,     0.1425
0.7046E-04,     0.1670
0.1385E-03,     0.1915
0.2489E-03,     0.2160
0.4182E-03,     0.2405
0.6658E-03,     0.2650
0.1016E-02,     0.2895
0.1495E-02,     0.3140
```

```
0.2137E-02,    0.3385
0.2978E-02,    0.3630
0.4063E-02,    0.3875
0.5440E-02,    0.4120
0.7168E-02,    0.4365
0.9312E-02,    0.4610
0.1195E-01,    0.4855
0.1516E-01,    0.5100
0.1904E-01,    0.5345
0.2372E-01,    0.5590
0.2932E-01,    0.5835
0.3598E-01,    0.6080
0.4390E-01,    0.6325
0.5327E-01,    0.6570
0.6435E-01,    0.6815
0.7742E-01,    0.7060
0.9283E-01,    0.7305
0.1110E+00,    0.7550
0.1326E+00,    0.7795
0.1581E+00,    0.8040
0.1885E+00,    0.8285
0.2251E+00,    0.8530
0.2696E+00,    0.8775
0.3245E+00,    0.9020
0.3941E+00,    0.9265
0.4866E+00,    0.9510
0.6225E+00,    0.9755
0.7278E+00,    0.9877
0.1000E+01,    1.0000
*MOISTURE SWELLING
0.0,0.20
0.0,0.50
0.0,0.626
1.765E-3,0.70
4.151E-3,0.80
6.537E-3,0.90
8.923E-3,1.00
*SOLID SECTION,ELSET=CONCRETE,MATERIAL=MAT4
*MATERIAL,NAME=MAT4
*ELASTIC
2.5E+04,0.167
*POROUS BULK MODULI
4.0E4,2.0E3
*PERMEABILITY, SPECIFIC=0.01
1.0E-14,0.695
*DENSITY
2300.0E-6
*EXPANSION
1.0E-05
*EXPANSION, PORE FLUID
1.667E-4
**
*INITIAL CONDITIONS, TYPE=TEMPERATURE
NTOT, 15.0
*INITIAL CONDITIONS, TYPE=RATIO
NTOT, 0.695
*INITIAL CONDITIONS, TYPE=SATURATION
NBENT, 0.626
NCONC, 1.00
*INITIAL CONDITIONS, TYPE=PORE PRESSURE
```

```
NBENT, -15.43
NCONC, 0.0
*AMPLITUDE, NAME=H3
0.0,1.0,1.0E15,1.0
**
** Constrain left and bottom boundary against normal displacement
**
*BOUNDARY
LEFT,1
BOT_DIS,2
**
** Fix fluid pressure to zero along outer boundaries
**
RIGHT_FL,8
BOT_FL,8
TOP_FL,8
***
*** Run Transient Analysis
***
***
*** Step 1a: To end of first second - apply gravity loading only
***
*STEP, INC=2000
*SOILS, CONSOLIDATION, UTOL=1000.0
1.0E-2,1.0,1.0E-4
*DLOAD,AMPLITUDE=H3
ELTOT,GRAV,9.81,0,-1
TOP1,P3,0.0
RIGHT1,P2,0.0
*RESTART, WRITE, FREQUENCY=5000
*NODE PRINT,FREQUENCY=0
*EL PRINT,FREQUENCY=0
*EL FILE,ELSET=ELOUTPT,FREQUENCY=1,POSITION=AVERAGED AT NODES
S,SAT,POR,VOIDR
*END STEP
***
*** Step 1b: To end of two seconds - apply fluid pressure to gap
***
*STEP, INC=2000
*SOILS, CONSOLIDATION, UTOL=1000.0
1.0E-2,1.0,1.0E-4
*BOUNDARY, AMPLITUDE=H3
CRACK,8,,0.05
*RESTART, WRITE, FREQUENCY=5000
*NODE PRINT,FREQUENCY=0
*EL PRINT,FREQUENCY=0
*EL FILE,ELSET=ELOUTPT,FREQUENCY=1,POSITION=AVERAGED AT NODES
S,SAT,POR,VOIDR
*END STEP
**
*** Step 1c: To end of first hour - input nodal temperature values
***
*STEP, INC=2000
*SOILS, CONSOLIDATION, UTOL=1000.0
0.1,3.6E3
*TEMPERATURE, FILE=tc3a2gio, BSTEP=1, ESTEP=1
**
*RESTART, WRITE, FREQUENCY=5000
*NODE PRINT,FREQUENCY=0
*EL PRINT,FREQUENCY=0
```

```
*EL FILE,ELSET=ELOUTPT,FREQUENCY=1,POSITION=AVERAGED AT NODES
S,SAT,POR,VOIDR
*END STEP
***
*** Step 2: To end of first day
***
*STEP, INC=2000
*SOILS, CONSOLIDATION, UTOL=1000.0
1.0E2,8.28E4
*TEMPERATURE, FILE=tc3a2gio, BSTEP=1, ESTEP=2
*RESTART, WRITE, FREQUENCY=5000
*NODE PRINT,FREQUENCY=0
*EL PRINT,FREQUENCY=0
*EL FILE,ELSET=ELOUTPT,FREQUENCY=1,POSITION=AVERAGED AT NODES
S,SAT,POR,VOIDR
*END STEP
***
*** Step 3: To end of first month
***
*STEP, INC=2000
*SOILS, CONSOLIDATION, UTOL=1000.0
1.0E2,2.5056E6,,8.64E4
*TEMPERATURE, FILE=tc3a2gio, BSTEP=2, ESTEP=5
*RESTART, WRITE, FREQUENCY=5000
*NODE PRINT,FREQUENCY=0
*EL PRINT,FREQUENCY=0
*EL FILE,ELSET=ELOUTPT,FREQUENCY=1,POSITION=AVERAGED AT NODES
S,SAT,POR,VOIDR
*END STEP
***
*** Step 4: To end of fifth month
***
*STEP, INC=2000
*SOILS, CONSOLIDATION, UTOL=1000.0
1.0E3,1.0368E7,,8.64E4
*TEMPERATURE, FILE=tc3a2gio, BSTEP=5, ESTEP=17
*RESTART, WRITE, FREQUENCY=5000
*NODE PRINT,FREQUENCY=0
*EL PRINT,FREQUENCY=0
*EL FILE,ELSET=ELOUTPT,FREQUENCY=1,POSITION=AVERAGED AT NODES
S,SAT,POR,VOIDR
*END STEP
```

APPENDIX C

TABULAR OUTPUT FROM ABAQUS FOR THE TC3 PROBLEM

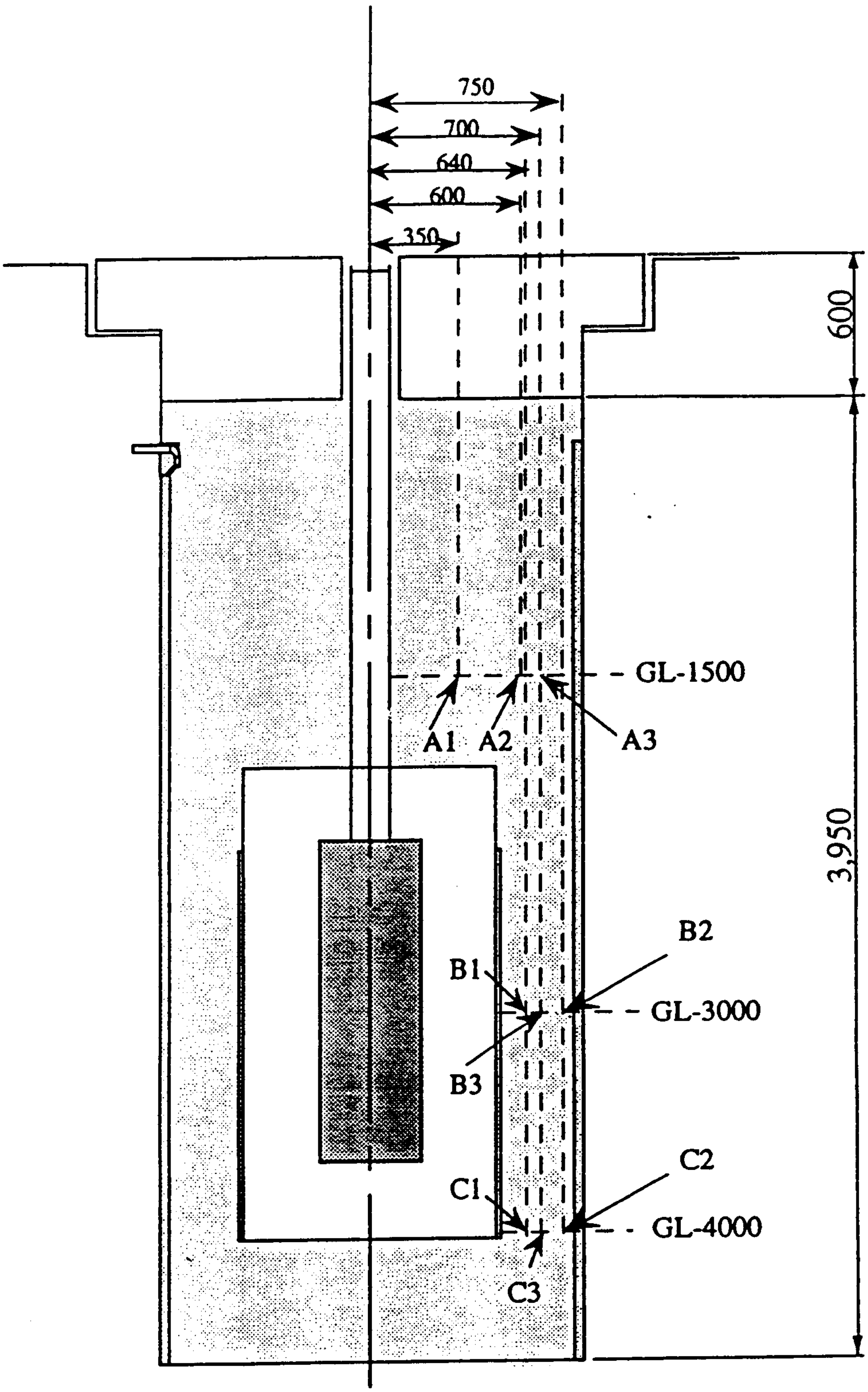

Figure C–1. Location of output monitoring points (Dimensions: mm)

Table C-1. Output results from ABAQUS at various points within the bentonite.

(a) After 1 month

Point	T (°C)	θ (%)	σ_z (MPa)*	σ_r (MPa)*
A1	27.90	26.1	-0.965	-1.187
A2	26.12	26.1	-1.037	-1.164
A3	25.17	26.1	-1.034	-1.154
B1	44.32	26.6	-1.614	-2.148
B2	39.27	26.2	-1.405	-1.818
B3	41.68	26.5	-1.595	-2.110
C1	38.93	26.4	-1.315	-1.838
C2	34.46	25.9	-1.149	-1.451
C3	36.52	26.4	-1.324	-1.759

(a) After 5 months

Point	T (°C)	θ (%)	σ_z (MPa)*	σ_r (MPa)*
A1	38.12	26.8	-1.910	-2.376
A2	36.05	26.8	-1.994	-2.228
A3	34.94	33.3	-0.923	-0.572
B1	55.41	29.4	-2.576	-3.402
B2	50.16	39.3	-0.261	0.133
B3	52.68	34.1	-1.650	-1.966
C1	49.57	28.8	-2.113	-2.965
C2	44.81	39.6	0.138	0.728
C3	47.01	33.8	-1.271	-1.479

* Compressive stresses negative (Note: Stresses listed above are effective stresses)

Variables:

T - Temperature
θ - Volumetric water content
σ_z - Vertical stress component
σ_r - Radial stress component